

1 **The proteomic inventory reveals the chloroplast ribosome as nexus within a**
2 **diverse protein network**

3

4

5 Lisa Désirée Westrich¹, Vincent Leon Gotsmann¹, Claudia Herkt¹, Fabian Ries¹,
6 Tanja Kazek¹, Raphael Trösch¹, Silvia Ramundo², Jörg Nickelsen³, Laura
7 Armbruster⁴, Markus Wirtz⁴, Zuzana Storchová⁵, Markus Raeschle⁵ and Felix
8 Willmund^{1*}

9

10 Author's institution(s)/affiliation(s):

11 ¹ Molecular Genetics of Eukaryotes, University of Kaiserslautern, Paul-Ehrlich-Str.
12 23, 67663 Kaiserslautern, Germany.

13 ² Department of Biochemistry and Biophysics, University of California, 600 16th St,
14 N316, San Francisco, CA 94143, USA.

15 ³ Department of Molecular Plant Science, University of Munich, Grosshaderner-Str.
16 2-4, 82152 Planegg-Martinsried, Germany.

17 ⁴ Centre for Organismal Studies, University of Heidelberg, Im Neuenheimer Feld 360,
18 69120 Heidelberg, Germany.

19 ⁵ Molecular Genetics, University of Kaiserslautern, Paul-Ehrlich-Str. 24, 67663
20 Kaiserslautern, Germany.

21

22 ***Corresponding author:** Felix Willmund (willmund@bio.uni-kl.de)

23 **ONE-SENTENCE SUMMARY:**

24 Affinity purification of *Chlamydomonas reinhardtii* chloroplast ribosomes and
25 subsequent proteomic analysis revealed a broad spectrum of interactors ranging
26 from global translation control to specific pathways.

27

28 **SHORT TITLE:** The chloroplast ribosome interaction network

29 **ABSTRACT:**

30 Chloroplast gene expression is tightly regulated and majorly controlled on the level of
31 protein synthesis. Fine-tuning of translation is vital for plant development, acclimation
32 to environmental challenges and for the assembly of major protein complexes such
33 as the photosynthesis machinery. However, many regulatory mediators and the
34 interaction network of chloroplast ribosomes are not known to date. We report here
35 on a deep proteomic analysis of the plastidic ribosome interaction network in
36 *Chlamydomonas reinhardtii* cells. Affinity-purification of ribosomes was achieved via
37 endogenous affinity tagging of the chloroplast-encoded protein Rpl5, yielding a
38 specific enrichment of >650 chloroplast-localized proteins. The ribosome interaction
39 network was validated for several proteins and provides a new source of mainly
40 conserved factors directly linking translation with central processes such as protein
41 folding, photosystem biogenesis, redox control, RNA maturation, energy and
42 metabolite homeostasis. Our approach provided the first evidence for the existence
43 of a plastidic co-translational acting N-acetyltransferase (cpNAT1). Expression of
44 tagged cpNAT1 confirmed its ribosome-association, and we demonstrated the ability
45 of cpNAT1 to acetylate substrate proteins at their N-terminus. Our dataset
46 establishes that the chloroplast protein synthesis machinery acts as nexus in a highly
47 choreographed, spatially interconnected protein network and underscores its wide-
48 ranging regulatory potential during gene expression.

49 **INTRODUCTION:**

50 Protein synthesis, or translation is the process by which the genetic information is
51 decoded from linear nucleic acid strands into diverse three-dimensional protein
52 structures. This process is achieved through ribosomes, the highly abundant
53 macromolecular ribonucleoprotein machinery present in all kingdoms of life. The core

54 components of ribosomes, responsible for the tasks of decoding the messenger RNA
55 (mRNA) and for the condensation of polypeptide bonds, are highly conserved. Also
56 the large rRNA molecules and the mainly positively charged ribosomal proteins are
57 overall well preserved. However, the exact composition and architecture of
58 ribosomes is highly flexible and may drastically vary between species or even within
59 cells (Roberts et al., 2008; Petrov et al., 2014). This is consistent with the “ribosome
60 filter hypothesis” by Mauro and Edelman (Mauro and Edelman, 2002, 2007), which
61 states that ribosomal populations are not uniform but rather diverse in terms of
62 composition, and dynamic in order to serve the translation of a specific
63 spatiotemporal mRNA pool. Their central role at the interface between the genetic
64 realm (transcription of the static genomic information, mRNA maturation and
65 turnover) and the highly adaptive proteome (protein maturation, modification and
66 turnover) make ribosomes central hubs of extensive regulation (Pechmann et al.,
67 2013; Stein and Frydman, 2019). In fact, regulation occurs during all steps of protein
68 synthesis, including translation initiation, elongation, modulation of translation-
69 competent ribosome pools and nascent polypeptide processing (Preissler and
70 Deuerling, 2012; Gloge et al., 2014; Hinnebusch, 2015; Stein and Frydman, 2019;
71 Trösch and Willmund, 2019; Waudby et al., 2019). The regulatory network dedicated
72 for this task is intriguingly complex, and many details are poorly understood to date.
73 The need for rapid adjustments of this central step becomes apparent by considering
74 that translation accounts for ~50% of the energy consumption in bacterial cells
75 (Russell and Cook, 1995) and that >10% of all proteins are thought to contribute to
76 translation at various levels (Costanzo et al., 2000).

77 In plants, ribosomes are found in three subcellular compartments, the cytosol,
78 chloroplasts and mitochondria. Due to their prokaryotic origin (Gray, 1993),
79 organelles perform protein synthesis via bacterial-type 70S ribosomes, which are

80 composed of a small 30S and a large 50S subunit. However, both chloroplast and
81 mitochondrial ribosomes specifically adapted to their organellar task and substantially
82 increased in molecular weight after the endosymbiotic event (Barkan, 2011; Zoschke
83 and Bock, 2018). Like *E. coli* ribosomes, chloroplast ribosomes contain an equivalent
84 set of rRNAs (5S, 16S and 23S rRNAs) that function as scaffold for ribosome
85 biogenesis (Maier et al., 2013), as peptidyl transferase and decoding unit. However,
86 the 23S rRNA gene is split in two parts, the mature rRNA is fragmented and some
87 plastid-specific rRNA secondary structures were described (Whitfield et al., 1978;
88 Bieri et al., 2017; Zoschke and Bock, 2018). The proteinaceous part of plastidic
89 ribosomes diversified from prokaryotic ribosomes, which led to a loss of Rpl25 and
90 Rpl30 in most plant species and an acquisition of so-called “plastid-specific ribosomal
91 proteins” (PSRPs) (Zoschke and Bock, 2018). About one third of all chloroplast
92 ribosomal proteins are encoded by the chloroplast genome (plastome), whereas the
93 remaining proteins are post-translationally imported from the cytosol. Similarly,
94 multiple other major chloroplast complexes exhibiting photosynthesis or gene
95 expression functions contain complex subunits of both genetic origins (e.g. Maul et
96 al., 2002). For the orchestration of complex assembly combining these subunits,
97 plastidic gene expression is subject to substantial regulation. Such coordination and
98 the need to quickly respond to environmental cues is achieved by predominant post-
99 transcriptional and translational regulation strategies (Eberhard et al., 2002; Zoschke
100 and Bock, 2018). Major players in this regulation belong to a group of nuclear-
101 encoded ‘Organelle Trans-Acting Factors’ that control maturation and stability of
102 plastidic transcripts (so-called M factors) and translation activation (so-called T
103 factors). Over recent years, several of these proteins were described and mainly
104 exhibit specific functions during the expression of one specific target transcript
105 (Nickelsen et al., 2014). Co-translational regulation of the protein synthesis rates

106 might be the key step for fine-tuning gene expression in chloroplasts. For example,
107 only mild changes of transcript levels, but profound changes in protein synthesis
108 were observed upon day and night cycles, environmental alteration (Sun and Zerges,
109 2015; Chotewutmontri and Barkan, 2018; Schuster et al., 2019), and during plant
110 development (Chotewutmontri and Barkan, 2016). Furthermore, several ribosome
111 profiling approaches of chloroplast translation reported severely fluctuating
112 elongation speed over individual open reading frames interrupted by short pauses,
113 which may reflect processing or insertion of nascent polypeptides into the thylakoid
114 membrane (Zoschke et al., 2013; Zoschke and Barkan, 2015; Chotewutmontri and
115 Barkan, 2018; Gawronski et al., 2018; Trösch et al., 2018). All these findings point to
116 the involvement of several factors that regulate translation in chloroplasts. However,
117 the regulatory network within the complex cellular milieu remains elusive and
118 demands for an in-depth proteomic analysis.

119 Here, we investigated the extent and components of the chloroplast ribosome
120 interaction network in *Chlamydomonas reinhardtii* (*Chlamydomonas* hereafter). By
121 specifically engineering an affinity tag into one of the chloroplast-encoded ribosomal
122 proteins, we were able to overcome caveats of other ribosome isolation protocols.
123 For example, classical approaches such as isolation of high-molecular weight
124 polysomal particles from sucrose gradient fractions yield mixed populations of
125 cytosolic, mitochondrial and plastidic ribosomes and unspecific high-molecular weight
126 complexes that co-migrate in gradients. Endogenous expression of tagged Rpl5
127 allowed us to perform affinity purification-mass spectrometry (AP-MS), in which
128 ribosome composition and their interaction network were specifically determined by
129 mass spectrometry. We revealed a surprisingly high number of proteins of known
130 and unknown function that associate with chloroplast ribosomes. Several of these
131 proteins were newly annotated, based on their homology to proteins of other

132 compartments, bacteria or higher plants. Within the pool previously unknown proteins
133 we discovered an N-acetyltransferase which was characterized in more detail. By this
134 we could provide the first evidence that co-translation N-acetylation of nascent
135 polypeptides occurs in chloroplast.

136 **RESULTS AND DISCUSSION:**

137 **Strategy for the targeted Isolation of Chloroplast Ribosomes**

138 Early proteomic analyses of purified chloroplast ribosomes from *Chlamydomonas*
139 and spinach led to the first identification of the core-component of this protein
140 synthesis machinery and a handful of regulatory factors (e.g. Beligni et al., 2004).
141 However, the overall network involved in translation regulation remained obscure,
142 mainly because of challenges such as the transient nature of the translation process,
143 the preparative difficulty to quickly separate cytosolic from chloroplast ribosomes and
144 the limited sensitivity of mass spectrometers, which need to detect low abundant,
145 regulatory proteins in complex protein samples containing highly abundant ribosomal
146 proteins. These can be overcome by affinity purification of ribosomes by introducing
147 a tag at the endogenous locus which is feasible for chloroplast-encoded genes in
148 *Chlamydomonas*. We thus screened the available high-resolution structures of the
149 plastidic ribosomes (e.g. Bieri et al., 2017; Boerema et al., 2018) for chloroplast-
150 encoded ribosomal subunits that have a surface exposed and accessible C-terminus.
151 Rpl5 (uL5c hereafter (Ban et al., 2014)) was one of the few proteins that seem suited
152 for this strategy, since it is situated at the interface between the 30S and 50S subunit,
153 next to 30S head (Figure 1A). For endogenous integration into the plastome, via
154 homologous recombination, the coding sequence of uL5c including the C-terminal
155 addition of a triple-hemagglutinin (HA) affinity tag was cloned adjacent to the Spec^R
156 resistance marker gene *AadA* (Goldschmidt-Clermont, 1991) (Figure 1B, top panel).

157 Upon several rounds of selection on plates with increasing concentrations of
158 spectinomycin, correct integration of the 3xHA sequence and homoplasmy was
159 verified by PCR. In all tested L5-HA lines, PCR fragments corresponding to the
160 smaller size of the non-tagged wild-type version were not detectable anymore, which
161 suggests that all copies of the plastome carried tagged uL5c (Figure 1B, bottom left).
162 Immunoblots with monoclonal anti-HA antibodies showed a specific signal at an
163 apparent molecular weight of 24-25 kDa in the L5-HA strains (Figure 1B, bottom
164 right). In *E. coli*, uL5 is an essential protein (Shoji et al., 2011). We hence tested if the
165 3xHA interferes with the uL5c function in chloroplasts. However, we did not detect
166 any proliferation differences between wild-type and L5-HA strains grown under
167 photoautotrophic conditions (Figure 1C). Furthermore, polysome analysis of a L5-HA
168 strain via sucrose gradients showed that the ribosomal proteins uL5c-HA, uL1c and
169 uS11c were all detectable in higher molecular weight fractions. This indicates that
170 tagged chloroplast ribosomes are competent for translation (Figure 1D).

171 **Functionally Intact Ribosomes can be Analyzed by AP-MS**

172 In our previous study on the plastidic ribosome-associated molecular chaperone
173 “trigger factor” (TIG1), we observed that chloroplast ribosome-nascent chain
174 complexes (RNCs) are instable during sample preparation (Rohr et al., 2019).
175 Pretreatment with chloramphenicol (a drug arresting elongation of 70S ribosomes)
176 and brief *in vivo* crosslinking with 0.37% formaldehyde helped to preserve the
177 interactions (Rohr et al., 2019). Consequently, similar conditions were used for all
178 AP-MS analyses. After harvest, lysates were treated with 1% of the detergent n-
179 Dodecyl- β -D-maltoside (DDM) in order to yield both ribosome interactors of the
180 soluble stroma fraction and at thylakoid membranes. All experiments were conducted
181 in parallel with the L5-HA strains and the untagged parent wild type as control (Figure
182 2A). We initially tested if affinity purifications yielded pure and functional RNCs.

183 Immunoblots of pulldown eluates from L5-HA and the wild-type lysates showed that
184 proteins of the 50S (uL1c) and 30S (uS11c) chloroplast ribosomal subunits co-
185 purified with L5-HA, whereas uL37, a protein of the 60S cytosolic ribosomal subunit,
186 was not detectable (Figure 2B). Importantly, the two known chloroplast ribosome-
187 associated nascent chain processing factors TIG1 and cpSRP54 also specifically co-
188 eluted in L5-HA pulldowns indicating that the approach yielded intact RNCs (Figure
189 2B). Except a weak background of uL1c, no signal was detectable for all tested
190 proteins within pulldown eluates from untagged cells.

191 For a deeper coverage of identified proteins via mass spectrometry, the bulk
192 of ribosomal proteins was separated from other proteins via SDS-PAGE and
193 analyzed separately (see Methods). Overall, more than 4200 proteins were identified
194 in the eluates of either the L5-HA or wild-type samples (Supplemental Dataset 1).
195 Importantly, biological replicates were highly reproducible with R^2 values >0.86
196 (Supplemental Figure 1). Using a modified t -test with a permutation-based false
197 discovery rate cut-off ($FDR < 0.05$, $S_0 = 1$), 850 proteins were found to be significantly
198 enriched in the L5-HA pull-down compared to control pull-downs carried out with the
199 wild-type strain. Importantly, all 52 subunits of the chloroplast ribosome were readily
200 detected. Of those, 24 unique peptides covering 97.7% of the chloroplast-encoded
201 Rpl23 were determined, which demonstrates that uL23c is not a pseudogene in
202 *Chlamydomonas* as in some other plants such as species of the Caryophyllidae and
203 Rosidae families (Moore et al., 2010). While proteins of the large chloroplast
204 ribosome subunit were on average 10-fold enriched over the control pulldown, the
205 mean enrichment of the small subunit was only 2.5-fold (Figure 2C, dark and light
206 green, respectively). This is likely due to the fact that the anti HA antibody efficiently
207 targeted both the assembled 70S ribosome as well as the free 50S pool only, but not
208 the pool of the free the 30S. Most importantly, virtually all ribosomal proteins of the

209 cytosolic 80S and the mitochondrial 70S particles were not enriched in the L5-HA
210 pulldowns (Figure 2C). Given the high abundance and general “stickiness” of these
211 ribosomal proteins, this further demonstrates the high selectivity of our quantitative
212 AP-MS approach. In addition, the significantly enriched proteins were predominantly
213 annotated with a localization in the chloroplast (i.e. 79% plastidic, 9% mitochondrial,
214 11% cytosolic, 1% others; Figure 2D and Supplemental Figure 3), further suggesting
215 that we were able to trap fully functional ribosome assemblies together with their
216 tightly associated auxiliary factors that facilitate protein translation in the chloroplast.

217 **Functional Categories of Factors Involved in the Ribosome Interaction Network**

218 Remarkably, many factors belonging to the ribosome interaction network show a high
219 conservation within the green lineage compared to other processes in the
220 *Chlamydomonas* chloroplast: ~70% of all enriched chloroplast ribosomal proteins
221 have orthologous forms in the land plant *Arabidopsis thaliana* (*Arabidopsis*)
222 compared to an average of 52% conserved proteins for the whole *Chlamydomonas*
223 chloroplast proteome (Figure 2E). For better classification, we functionally assigned
224 all proteins that were significantly enriched in the L5-HA dataset. This classification
225 was based on the most recent genome annotation (v5.6), the annotation of
226 orthologous proteins of *Arabidopsis* or BLAST search (see Methods). Besides the
227 expected categories of translation regulation, ribosome biogenesis, molecular
228 chaperones and proteases we also identified a number of other functional categories
229 such as RNA processing, redox signaling, post-translational modification (PTM) and
230 various metabolic pathways (Figure 2F), which will be briefly outlined in the sections
231 below. Importantly, many of the identified factors were previously not known to act in
232 the context of chloroplast translation (see below).

233 *Factors involved in translation regulation and ribosome biogenesis:*

234 Throughout all kingdoms of life, three stages of translation are described, which are
235 all regulated by a specific set of factors. In agreement with their prokaryotic origin,
236 chloroplast translation is regulated by prokaryotic-type factors (Zoschke and Bock,
237 2018). For chloroplast translation initiation in *Chlamydomonas*, we enriched all
238 canonical factors IF1, IF2 and IF3, which mediate initiator tRNA binding and subunit
239 assembly. In addition, we enriched the protein Cre06.g278264, a homolog to
240 AT3G43540, which is a plastidic *Arabidopsis* protein of unknown function that
241 contains a predicted IF4F domain. All four elongation factors (EF-Tu, cpEFT, EFG,
242 EFP) were enriched. We further enriched LEPA which shows homology to EFG.
243 Interestingly, bacterial LEPA/EF4 was shown to back-translocate tRNAs on the
244 ribosome, which might be important for elongation quality control (Qin et al., 2006).
245 The *Arabidopsis cplepa-1* mutants display photosynthesis defects, suggesting an
246 important role of LEPA during plastid protein synthesis (Ji et al., 2012). For
247 translation termination, we only found plastid release factor 1 (PRF1), which serves
248 for the release of transcripts with UAA/UAG stop codons, respectively. This is
249 consistent with previous studies that *opal* UGA stop codons are not used in the
250 chloroplast of *Chlamydomonas* (Young and Purton, 2016). In addition,
251 Cre01.g006150 was enriched, which shows homology to bacterial RF3 that facilitates
252 dissociation of RF1 from the ribosome (Beligni et al., 2004). Among the significant
253 outliers that are directly involved in the translation cycle were the ribosome recycling
254 factor RRF1 and a peptidyl-tRNA hydrolase (Cre02.g076600) that cleaves the ester
255 bond in the peptidyl-tRNA complex (Das and Varshney, 2006). Of the plastid-specific
256 ribosomal proteins (PSRPs), only PSRP1 was enriched. In fact, PSRP1 is no longer
257 considered to be a true “plastid-specific” protein. Rather, this protein displays
258 homology to the long hibernation promoting factor of some bacteria (Trösch and
259 Willmund, 2019). PSRP3 and 4, previously thought to act as integral component of

260 chloroplast ribosomes (Zoschke and Bock, 2018) were not enriched, which argues
261 against a genuine structural role of these proteins at least within algae. In addition to
262 PSRP1, further ribosome hibernation factors were identified in the dataset, such as
263 the ribosome silencing factor IoJAP and HFLX, an antagonist of bacterial hibernation
264 promoting factors (Basu and Yap, 2017). Ribosome hibernation in chloroplasts
265 remains enigmatic, since 100S ribosomes have not been observed so far, however,
266 the tuning of translation during diurnal cycles and the presence of these factors
267 points to the existence of similar processes in chloroplasts (reviewed in Trösch and
268 Willmund, 2019).

269 Members of the ATP-hydrolyzing ABC superfamily are highly conserved
270 across species and exhibit diverse functions (Murina et al., 2018; Ero et al., 2019).
271 Most subclasses within the ABC family carry transmembrane domains; however,
272 these are absent in the ABC-E and ABC-F sub-families (Kerr, 2004). Several factors
273 of such ABC-F domain containing superfamily were clearly enriched in the L5-HA
274 dataset with high LFQ scores (Figure 3A). Intriguingly, ABC-F proteins are
275 considered to directly act on ribosomes and play important roles during translation,
276 ribosome assembly and antibiotic resistance (Murina et al., 2018). The
277 *Chlamydomonas* genome encodes for several eukaryotic ABC-F members
278 (Supplemental Figure 4). Our phylogenetic analysis showed that all five bacterial-
279 type ABC-F proteins carry predicted chloroplast transit peptides and are also
280 enriched in the L5-HA dataset (Supplemental Figure 4). For example,
281 Cre07.g3335400 shares >55% identity to the energy-dependent translational throttle A
282 (EttA), which is postulated to regulate protein synthesis within energy-depleted cells
283 (Boel et al., 2014) (Figure 3A). Further proteins are members of the bacterial YbiT,
284 YheS and Uup classes (Murina et al., 2018). It can be assumed that these factors

285 also regulate chloroplast translation or promote resistance to translation-targeted
286 drugs in chloroplasts.

287 Biogenesis and assembly of chloroplast ribosomes is poorly understood, but
288 the conservation of a core set of ribosomal proteins from bacteria and chloroplasts
289 suggests that the process is similar to the well-characterized process in *E. coli*
290 (Kaczanowska and Ryden-Aulin, 2007; Maier et al., 2013). Most of the factors that
291 were co-purified in our L5-HA pulldown were ortholog to factors involved in late
292 biogenesis and maturation of the ribosomal subunits (Supplemental Dataset 1). For
293 example, Cre02.g145000 is ortholog to the cold shock protein RBF1 which is
294 essential for cell growth at low temperatures in *E. coli* and acts during late ribosome
295 maturation (Shajani et al., 2011). We also found a member of the GTPase RbgA
296 family, which is thought to control chloroplast ribosome biogenesis during
297 environmental stresses (Jeon et al., 2017). In addition, we could enrich
298 Cre01.g033832 which shows homology to *Arabidopsis* RH39. RH39 was postulated
299 to remove specific regions (hidden breaks) from the 23S rRNA (Nishimura et al.,
300 2010).

301 *tRNA maturation and charging and amino acid metabolism:*

302 Our ribosome interaction network comprised a number of tRNA maturation,
303 modification and charging factors. For many years, tRNA modification was
304 considered to occur exclusively during tRNA synthesis. However, there is
305 accumulating evidence that tRNA modification is highly dynamic and reversible and
306 directly influences tRNA selection at the ribosomal A-site, local elongation speed and
307 co-translational folding, which is adjusted in response to environmental cues
308 (reviewed in Krutyholowa et al., 2019). Among these modifying enzymes, we found
309 proteins containing tRNA pseudo-uridine synthase (PUS1, 3, 8, 9, 19) or
310 methyltransferase domains (TMU3, CGL27). Also two homologs of the bacterial

311 MnMEG pathway were found, which hyper-modify uridine 34 at the wobble position
312 of the tRNA (Armengod et al., 2014). In addition, we revealed many chloroplast tRNA
313 synthases, responsible for charging tRNAs (Supplemental Figure 5A). This agrees
314 with the situation within the cytosol where all tRNA synthases of the multi-ARS
315 complex co-migrated with polysomes and thus seem to optimize protein synthesis by
316 channeling tRNAs directly to ribosomes (David et al., 2011). Surprisingly we co-
317 purified a remarkable number of enzymes, which are involved in different steps of
318 amino acid biosynthesis (Supplemental Dataset 1). This suggests that, at least in the
319 chloroplast, where most of the amino acids are synthesized in plant cells, translation
320 is spatially coupled with amino acid supply. This finding goes in hand with earlier
321 studies using flux balance analysis which showed that translation efficiency and
322 ribosome density on translated transcripts positively correlates with amino acid
323 supply (Hu et al., 2015).

324 *Nascent chain folding and processing*

325 Molecular chaperones and nascent polypeptide modifying enzymes act early during
326 protein biogenesis. In bacteria, one of the first steps of nascent chain processing is
327 the co-translational removal of the formyl group from N-terminal formyl-methionine,
328 which is catalyzed by the metalloprotease termed peptidyl deformylase (PDF).
329 Subsequently, N-terminal methionines are frequently removed through essential
330 Methionine Aminopeptidase (MAP) which is found in all kingdoms of life (reviewed in
331 Gloge et al., 2014). We co-purified both a chloroplast variant of PDF (PDF1B) and
332 the MAP-related protein MAP1D in our ribosome pulldown. For early folding of
333 emerging nascent polypeptides, we found a surprisingly diverse set of molecular
334 chaperones including TIG1, two HSP70s, the co-chaperone CDJ1, the CPN60
335 chaperonin complex, HSP90C and the HSP100 family protein CLPB3, which were all
336 detected in the pulldown with high LFQ values (Figure 3B) (see below). In bacteria,

337 TIG1 is the main ribosome associated chaperone, which is partially assisted by the
338 Hsp70 DnaK (reviewed in Gloge et al., 2014). However, the co-translational
339 chaperone network in chloroplasts rather mirrors the cytosolic chaperone network
340 (Pechmann et al., 2013), which is a remarkable diversification from the chloroplast
341 ancestors and might be an essential adaptation for processing of the more complex
342 proteome topology within plant organelles.

343 *Protein targeting to chloroplast membranes*

344 About half of the chloroplast-encoded proteins are integral components of the
345 thylakoid membranes. Ribosome profiling studies in maize showed that protein
346 synthesis of approximately half of these nascent polypeptides initiate in the stroma
347 and that ribosomes relocate to membranes once the first transmembrane domain
348 emerges from ribosomes (Zoschke and Barkan, 2015). Similar to other systems, this
349 co-translational sorting cascade includes the chloroplast signal recognition particle
350 cpSRP54, which was shown to bind to plastidic ribosomes for sorting of a specific set
351 of thylakoidal membrane proteins (Hristou et al., 2019), the SRP receptor FTSY, and
352 the translocases SECY and ALB3 (a homolog of bacterial YidC) (reviewed in Ziehe et
353 al., 2017). However, little information about the co-translational pathway and its
354 components exists to date. In addition to cpSRP54, we found that plastidic ribosomes
355 interact with cpFTSY, STIC2, cpSECY1 and ALB3.2, one of the two ALB3 integrases
356 of *Chlamydomonas* (Figure 3C). Importantly, ALB3.2 was previously shown to be
357 important for the biogenesis of the Photosystem I and II (PSI/II) reaction centers,
358 while ALB3.1 rather integrates post-translationally imported proteins such as the light
359 harvesting complex (Göhre et al., 2006). In that study, ALB3.2 did not co-migrate with
360 plastidic polysomes, however, it was postulated that the interaction might be too
361 transient to be detected in polysome assays (Göhre et al., 2006). Here, the use of
362 chemical crosslinking might have stabilized this interaction. Notably, in yeast the

363 mitochondrial YidC homolog Oxa1 has been detected in isolated polysomes (Hell et
364 al., 2001). Importantly, the specific enrichment of the SRP components and ALB3.2
365 but not ALB3.1 further supports the high specificity of our AP-MS approach. Our
366 ribosome interaction network also comprises SECA1, which seems to be important
367 for co-translational targeting of the chloroplast-encoded cytochrome *f* subunit (Röhl
368 and van Wijk, 2001). The chloroplast genome also encodes for two proteins of the
369 inner envelope (i.e. CemA and Ycf1) and an involvement of a second, inner
370 envelope-localized Sec machinery has been proposed (Zoschke and Barkan, 2015).
371 However, we did not identify ribosome association of this second machinery.

372 Additional proteins have been shown to assist in the integration of proteins
373 into organellar membranes. In the yeast cytosol, Get3 integrates tail-anchored
374 proteins into the membrane of the endoplasmic reticulum (Borgese and Fasana,
375 2011). Recently, a paralog, Get3b has been identified in *Arabidopsis*, and shown to
376 be localized in the chloroplast (Xing et al., 2017). Strikingly, Get3b was enriched ~4-
377 fold in our ribosome purification, suggesting that this pathway may be intimately
378 linked to protein biogenesis in chloroplasts. An alternative and intriguing possibility is
379 that GET3b acts as a reactive oxygen species-activated ribosome-associated
380 chaperone in chloroplasts. It has been previously demonstrated that a highly
381 oxidative environment leads to a reversible transition of the cytosolic Get3 from an
382 ATP-dependent targeting protein to an effective ATP-independent chaperone during
383 stress situations (Voth et al., 2014).

384 *Biogenesis of Photosystem I and II*

385 For the biogenesis of the major thylakoid complexes involved in photosynthesis,
386 several assembly factors were found: PAM68 is a membrane-bound protein involved
387 in co-translational chlorophyll insertion (Armbruster et al., 2010), LPA1,
388 CPLD28/LPA3 and TEF30 are assembly factors of PS II (reviewed in Theis and

389 Schroda, 2016); CGL59/Y3IP1 (Albus et al., 2010) and CGL71/PYG7 (Shen et al.,
390 2017) contribute to PS I biogenesis; CGLD22 (a homolog of *Arabidopsis* CGL160)
391 (Rühle et al., 2014) and CGLD11 assist the assembly of the ATP synthase (Grahl et
392 al., 2016) and CCB4 is an assembly factor of the *Cytb₆f* complex (Lezhneva et al.,
393 2008). However, we did not enrich for the core PSI/II or ATP synthase complex,
394 indicating that their assembly may not occur in direct proximity to translating
395 (thylakoid membrane-associated) ribosomes. Rather, assembly factors may shuttle
396 between the ribosome and their designated target complexes.

397 *Trans-acting factors*

398 Most of nuclear-encoded 'Organelle Trans-Acting Factors' belong to a family
399 containing a degenerated amino acid motif of tandem repeats termed tetra-, penta-
400 and octotricopeptide repeats (TPRs, PPRs, and OPRs), respectively (Barkan and
401 Small, 2014; Hammani et al., 2014). Members of the TPR group are present from
402 cyanobacteria to land plants and the domain is mainly involved in mediating protein-
403 protein interactions. PPR proteins are absent in prokaryotes, while there are >400
404 members found in most land plant species (Barkan and Small, 2014). In contrast, in
405 *Chlamydomonas* only 14 PPR proteins has been described so far. Instead, more
406 than 120 algal specific OPR proteins likely take over the task of regulating the
407 transcript maturation (M factors) and translation (T factors). Most of the currently
408 known factors exhibit high specificity for one or few mRNA targets during chloroplast
409 gene expression. Importantly, we could attribute a co-translational task for several of
410 these already characterized *trans*-acting factors (Supplemental Table 3). In addition,
411 we provide evidence here that at least 25 additional, non-characterized OPR
412 proteins, are expressed and seem to associate with translating chloroplast ribosomes
413 (Figure 3D and Supplemental Dataset 1). While a ribosome association is not
414 surprising for the T factors, the co-purification of M factors (involved in specific

415 intercistronic transcript processing or end trimming) might be unexpected. However,
416 there is accumulating evidence that transcript processing factors may additionally
417 promote translation of their target mRNA. For example, the helical repeat protein
418 PPR10 binds and defines the 5'UTR end of *atpH*, but also remodels the RNA
419 structure in a way that the Shine Dalgarno sequence of *atpH* is accessible for
420 ribosome binding (reviewed in Zoschke and Bock, 2018). Of note, most OPRs show
421 rather low enrichment and LFQ values, pointing to low abundance or transient
422 interactions with translating ribosomes, as expected for factors that promote the
423 initiation of translation for a specific subset of mRNA pools. Of the enriched OPRs,
424 11 proteins belong to the NCL class that seem to differ from other OPRs by lower
425 specificity to a certain chloroplast transcript. In fact the two NCL proteins, NCC1 and
426 NCC2 (Boulouis et al., 2015) showed the highest enrichment of OPR co-purification
427 in the dataset (16-fold and 4-fold respectively) (Figure 3D).

428 *RNA maturation*

429 Unlike in bacteria, where translation occurs already during ongoing transcription, the
430 coupling of these processes in chloroplasts is still under debate (reviewed in Zoschke
431 and Bock, 2018). We found four of the five bacterial-type RNA polymerase subunits
432 enriched in the L5-HA pulldown, which goes hand in hand with earlier studies in land
433 plants where ribosomal proteins and translation factors were linked to transcription
434 (Pfalz et al., 2006; Majeran et al., 2012). Furthermore, PNP1 was enriched, which is
435 a reversible polynucleotide polymerase that trims 3' ends of stem loops and adds
436 poly(A)-rich tails to some transcripts with missing stem loops (Germain et al., 2011).
437 Additional factors involved in transcript processing were candidates for RNA
438 methyltransferases and RNases, such as RNAseJ (Supplemental Figure 5B and
439 Supplemental Dataset 1). Since our purification might have co-purified nucleoid
440 particles, we looked for orthologous forms of the proteins that were described in the

441 proteomics study of maize nucleoids (Majeran et al., 2012). None of the orthologous
442 proteins involved in DNA stability and organization was enriched in our dataset.
443 Intriguingly, several DEAD domain-containing RNA helicases seem to act in proximity
444 to chloroplast ribosomes. One putative task of ribosome-associated RNA helicases in
445 chloroplasts might be their contribution for maintaining protein-RNA interactions, as
446 observed in prokaryotic cells and the cytosol (Owtrim, 2013). In addition, RNA
447 helicases are important for altering the RNA conformations during translation and
448 might be of particular need during environmental change such as temperature
449 change, which severely alters mRNA secondary structures.

450 *Factors involved in post-translational modifications*

451 In *Chlamydomonas* and other plants, several findings point to a tight coupling of
452 chloroplast translation with the diurnal dark/light cycles, which ensures that the highly
453 energy demanding process of protein synthesis is supplied with sufficient energy.
454 This control was postulated to be mediated by “biochemical light proxies” (BLPs),
455 comprising chlorophyll or intermediates of photosynthesis such as reduced
456 plastoquinone, reduced thioredoxin or ATP/ADP levels (reviewed in Sun and Zerges,
457 2015). The redox state directly influences transcriptional dynamics in chloroplasts,
458 and there are also ample hints for the redox-dependent regulation of translation
459 (reviewed in Rochaix, 2013). Here, we found several putative BLPs that may exhibit
460 the task of light-dependent regulation such as thioredoxins of the X-, Y- and F-type,
461 NTRC and ferredoxins (Supplemental Figure 5C). NTRC was already implicated in
462 the cascade controlling the synthesis of PsbD (Schwarz et al., 2007). In yeast,
463 thioredoxin was shown to protect ribosomes against aggregation via the
464 peroxiredoxin Tsa1 that exhibits chaperone function during oxidative stress (Trotter
465 et al., 2008). Orthologous mechanisms could be envisioned, for example through the
466 enriched peroxiredoxin PRX1 protecting or regulating chloroplast translation during

467 day and night. Such control of chloroplast translation is also consent with the
468 "colocation for redox regulation (CoRR) hypothesis", stating that individual organelles
469 need to sense and adjust their components based on the redox state of their own
470 bioenergetic membranes (Allen, 2003; Maier et al., 2013).

471 The three prolyl hydroxylases PFH11, PFH17 and PHX23 were enriched in
472 the ribosome pulldown and may regulate translation by introducing post-translational
473 hydroxyl modification of ribosomal proteins and the elongation factor EF-Tu as shown
474 for the cytosol and in prokaryotes, respectively (Scotti et al., 2014; Horita et al.,
475 2015). Other enriched proteins involved in post-translational modifications belong to
476 the classes of kinases, phosphatases (with unknown function so far) and
477 methyltransferases. SET-domain lysine methyltransferases were shown to introduce
478 site-specific lysine methylations into histones, ribosomal proteins and the large
479 subunit of the ribulose-1,5-bisphosphate carboxylase/oxygenase, RbcL (Raunser et
480 al., 2009).

481 *Other proteins*

482 A remarkable number of putative ribosome-associated proteins belonging to various
483 metabolic pathways such as starch, fatty acid, and nucleotide metabolism
484 (Supplemental Dataset 1) were enriched in the pulldown. This co-isolation seems
485 surprising, however, a similar report describing the ribosome interaction network in
486 mammalian cells found also several metabolic enzymes, especially of glucose
487 metabolism in proximity to ribosomes (Simsek et al., 2017). Also, there is
488 accumulating evidence in literature that several metabolic enzymes exhibit RNA
489 binding activity and thus actively contribute to gene expression, including the subunit
490 of the chloroplast-localized chloroplast puruvate dehydrogenase complex, DLA2
491 which also co-purified in our L5-HA pulldown (Bohne et al., 2013; Castello et al.,
492 2015) (Supplemental Dataset 1). In bacteria, ribosomes were shown to engage with

493 metabolic enzymes via quinary interaction of micromolar affinity. Such interactions
494 have a direct impact on metabolic activity since ribosomes were shown to both
495 activate and inactivate specific classes of enzymes (DeMott et al., 2017). Thus,
496 similar spatiotemporal relationships between protein synthesis and metabolic
497 pathways can be envisioned for chloroplasts.

498 **Validation of Selected Ribosome-associated Factors**

499 With the relatively high number of proteins that co-purified with chloroplast
500 ribosomes, we wondered whether *in vivo* crosslinking attached ribosomes via direct
501 or secondary interactions to large chloroplast complexes or protein networks.
502 However, direct comparison of the migration behavior of ribosomes in crosslinked
503 and non-crosslinked samples showed the very similar polysome-behavior of
504 chloroplast ribosomes (judged by uL1c immunoblotting) under both conditions
505 (Supplemental Figure 6A). Furthermore, our AP-MS from solubilized cells (including
506 membranes) did not enrich for subunits belonging to the abundant photosynthesis
507 machineries (i.e. PSI, II, *Cytb_{6f}*, CF_{0,1} ATPase) as expected if over-crosslinking
508 would tether the ribosome apparatus via biogenesis factors to these complexes. To
509 test the extent of complex stabilization via the crosslink, we applied crosslinker *in*
510 *vivo* and performed a parallel AP-MS experiment under conditions with high ionic
511 strength to strip off loosely associated proteins and puromycin to prevent indirect
512 interactions via the nascent polypeptide chain. Overall, we could still detect most
513 proteins in this pulldown, as expected due to crosslinked interactions, however, the
514 overall enrichment in the “high salt” pulldown was reduced compared to the
515 conditions under low salt concentrations (Supplemental Figure 6B, Supplemental
516 dataset 1). This indicates that not all interactions were crosslinked to full saturation.
517 Interestingly, we observed that in those L5-HA pulldown experiments which were
518 performed with high salt conditions, proteins of some categories were more depleted

519 than others (Supplemental Figure 6). For example, some of the *trans*-acting proteins
520 or enzymes catalyzing post-translational modifications were low or even undetectable
521 after high salt treatment. In contrast, translation factors, protein targeting factors, or
522 many metabolic enzymes showed similar scores like the ribosomal core proteins
523 (Supplemental Figure 6C). This might be explained by the different binding affinities
524 of the respective interactors.

525 We furthermore validated proteins for their ribosome association through
526 independent polysome assays. To this end, crosslinked samples were kept untreated
527 or were treated with RNase I in order to cleave polysomes via digesting their
528 commonly translated mRNA. By this, proteins binding to translating ribosomes should
529 shift towards the monosomal fractions upon RNase I treatment (scheme on top of
530 Figure 4). Indeed, immunoblot signals for the ribosomal proteins and the plastidic
531 chaperones HSP90C, HSP70B, CPN60A, the sorting factor SECA, the PSII
532 assembly factor TEF30 and the *trans*-acting factor RBP40 were reduced in the
533 polysomal fractions of RNase I-treated samples (Figure 4). Moreover, puromycin
534 treatment prior to polysome assays released nascent chain associated chaperones
535 from polysomes as expected for chaperones assisting co-translational folding
536 (Supplemental Figure 7) (Teter et al., 1999; Rohr et al., 2019). Interestingly, NTRC
537 was only detectable in fractions corresponding to monosomes or unassembled
538 ribosomal subunits, both in the treated and untreated samples (Figure 4). Thus,
539 NTRC may act on or control the pool of non-translating ribosomes. As a control, the
540 abundant CF₁ ATPase subunit AtpB was plotted. Despite its migration into high
541 molecular weight fractions in sucrose gradients, no profound shift was observed upon
542 RNase I treatment (Figure 4), which agrees with the data that AtpB is not enriched in
543 the L5-HA pulldown. Overall, we could confirm the ribosome-association of several
544 putative interactors by independent analyses. In addition, the control experiments

545 showed a rather moderate crosslinking under the conditions used, which is also
546 substantiated by the fact that many proteins with an unlikely ribosome-interaction
547 were not present in the dataset (see chapter above).

548 **Co-translational N-acetylation is Present in Chloroplasts**

549 In eukaryotic cells, one of the most frequently occurring protein modifications is N-
550 terminal acetylation (NTA), which can be mediated co- and post-translationally. In the
551 cytosol, co-translational NTA is catalyzed by a ribosome-associated complex
552 consisting of the three N^α-acetyltransferase subunits NatA/B/C. This complex targets
553 nascent polypeptides at the initiator methionine or the first amino acid if the N-
554 terminal methionine was cleaved shortly after emerging from the ribosomal exit
555 tunnel (Tsunasawa et al., 1985). Although the biological consequence of cytosolic
556 NTA has not been fully solved to date, it appears to contribute during stress response
557 and acclimation. In the chloroplast, NTA was reported to occur on several nuclear-
558 and plastid-encoded proteins (Lehtimäki et al., 2015). Modification of the nuclear-
559 encoded proteins may be achieved by cytosolic N^α-Acetyltransferases (NATs) or
560 upon import into plastids. In *Arabidopsis*, seven putative chloroplast-localized NATs
561 were identified. However, it was not clear whether NTA of chloroplast encoded
562 proteins is accomplished co- or post-translationally (Dinh et al., 2015; Lehtimäki et
563 al., 2015).

564 Strikingly, a NAT domain-containing protein, Cre14.g614750, which shows
565 homology to the *Arabidopsis* protein AT4G28030 (one of the 7 putative chloroplast
566 NATs; (Dinh et al., 2015)), was 4-fold enriched in our L5-HA ribosome-purification
567 dataset. Thus, we propose Cre14.g614750 to name cpNAT1. Since this is the first
568 identification of a ribosome-associated NAT in the chloroplast, we aimed to further
569 characterize cpNAT1. The full-length NAT sequence carrying a C-terminal triple HA
570 tag was expressed in *Chlamydomonas* cells (Supplemental Figure 8). Consistent

571 with a clear prediction of its N-terminal transit peptide via ChloroP and Predalgo,
572 (Emanuelsson et al., 1999; Tardif et al., 2012), immunofluorescence (IF) microscopy
573 confirmed chloroplast localization of cpNAT1-HA (Figure 5A). In fact, cpNAT1-HA
574 showed a highly similar localization pattern like chloroplast ribosomes (as indicated
575 by IF of uL1c). The strongest IF signal is adjacent to the pyrenoid, displaying similar
576 patterns like the T-zones, the spatiotemporal regions of photosystem biogenesis
577 (Sun et al., 2019). Next, we independently confirmed the ribosome-association of
578 cpNAT1 by ribosome co-sedimentation assays. Chemical crosslinking profoundly
579 enhanced the signal of cpNAT1-HA in ribosomal pellets. Importantly, dissociation of
580 RNCs by addition of puromycin fully abolished sedimentation of cpNAT (Figure 5B).
581 Of note, TIG1 is not fully abolished under these conditions, since the protein might
582 directly interact with ribosomes (Rohr et al., 2019).

583 *Chlamydomonas* mature cpNAT1, lacking the predicted transit peptide, shares
584 only 15% amino acid identity and 25% amino acid similarity with its mature
585 counterpart in *Arabidopsis* (Supplemental Figure 9). The most obvious difference is
586 an additional domain of 135 residues constituting the N-terminus of the mature
587 protein, which seems to be highly disordered (Figure 5C, top). Accordingly, we were
588 only able to create a homology model for the C-terminal NAT domain containing
589 residues Val142 to Leu328. This C-terminal domain includes the conserved acetyl-
590 CoA binding motif RxxGxG/A (Supplemental Figure 9). Modelling of this domain with
591 two online resources (RaptorX and SWISS-MODEL), matched well with several N-
592 acetyltransferases structures belonging to the GNAT-domain containing superfamily
593 (Figure 5C bottom and Supplemental Table 4). We thus asked, if the N-terminal part
594 is present in the mature form in chloroplasts. In fact, the tagged cpNAT-HA protein
595 migrates with an apparent molecular weight of 32 kDa in SDS gels, which is smaller
596 than the expected size of 44.3 kDa (including the HA tag). For comparison,

597 heterologously expressed and purified protein covering the full mature cpNAT1
598 sequence (with no transit peptide and no tag) migrates with an apparent molecular
599 weight of 37 kDa (Supplemental Figure 10). In addition, we could only detect
600 peptides covering the C-terminal NAT domain in our mass-spectrometric analysis
601 (Supplemental Figure 9). Hence, it is tempting to speculate that in *Chlamydomonas*,
602 cpNAT1 is further processed upon translocation into chloroplast.

603 In order to determine if cpNAT1 indeed exhibits N^α-acetylation activity, we
604 purified the predicted mature cpNAT1 after heterologous expression in *E. coli*. As
605 model substrate, we selected a peptide covering the N-terminal amino acids MTIA of
606 PsbD, which are conserved in PsbDs of *Chlamydomonas* and *Arabidopsis*. This
607 peptide sequence closely resembles the consensus sequence of N-terminally
608 acetylated proteins that are encoded in the plastome (Dinh et al., 2015). In the
609 absence of the ribosome, the specific activity of the purified mature cpNAT1 on this
610 model substrate was 216 ± 45 pmol min⁻¹ mg⁻¹ (Figure 5D). The N-terminal
611 acetylation of the substrate was strictly dependent on incubation time and the amount
612 of purified enzyme (Supplemental Figure 11). Hence, our results substantiate that co-
613 translational NTA exists in chloroplast, and that cpNAT1 might be the enzyme
614 responsible for modifying the previously reported proteins PsbA, PsbD, PsbC and
615 RbcL - all major subunits of the light and dark cycles reactions of photosynthesis.
616 The importance of co-translational N^α-acetylation for the protein fate remains to be
617 fully established in chloroplasts. However, a global proteomics study uncovered N-
618 terminal acetylation as the most frequent modification of stromal proteins in
619 *Chlamydomonas* and evidenced that NTA of stromal proteins positively correlates
620 with their stability (Bienvenut et al., 2011). In *Arabidopsis*, NTA of stromal proteins is
621 also frequent but the role of NTA to affect N-degron pathways is not established yet
622 (Zybailov et al., 2008; Rowland et al., 2015; Bouchnak and van Wijk, 2019). In

623 *Citrullus lanatus*, the N^α-acetylated form of the chloroplast-encoded ATP synthase
624 subunit AtpE is more resistant against proteolysis during drought stress when
625 compared with the non-acetylated proteoform (Hoshiyasu et al., 2013). Remarkably,
626 the abundance of cytosolic ribosome-associated NatA complex is tightly regulated by
627 the drought stress-related hormone ABA transduces the response towards drought
628 (Linster et al., 2015). NTA of cytosolic proteins by the ribosome-associated
629 complexes NatA and NatB is also essential for the responses towards pathogen-
630 attack or high salt stress (Huber et al., 2019). Based on these results, NTA is
631 supposed to control diverse stress responses in plants (Linster and Wirtz, 2018).
632 Thus, it will be intriguing to investigate if cpNAT1 contributes to stress adaptation in
633 chloroplasts by imprinting of plastome-encoded proteins with acetylation marks.

634 **CONCLUSIONS**

635 For many years, most proteomic studies of ribosomes focused on the identification of
636 core components or tightly associated factors of ribosomal particles. However, this
637 study and a recent study in mammalian cells (Simsek et al., 2017) demonstrate that
638 the ribosome interaction network is highly diverse, comprising several hundred
639 proteins of different functional pathways. This goes well beyond the *bona fide* list of
640 factors that govern the three major phases of protein synthesis (i.e. initiation,
641 elongation and termination) and the folding of emerging polypeptides (e.g. molecular
642 chaperones). The high degree of interconnectedness is not surprising given the high
643 abundance of ribosomes in the complex and tight environment of a cell. In
644 logarithmically growing *E. coli* cells, up to 70,000 70S ribosomes exist that make up
645 to 1/3 of the dry mass of the whole cell and a concentration of 70 μM
646 (<http://book.bionumbers.org>). Thus, ribosomes present a large surface for numerous
647 interactions. Recently, in-cell NMR spectroscopy showed that ribosomes engage in

648 several quinary interactions and they might directly - maybe even in a non-translating
649 fashion - affect several biochemical processes in a cell (DeMott et al., 2017). In
650 addition, ribosomes are highly dynamic and may exhibit spatiotemporal compositions
651 that even vary within a single ribosome population and which is dedicated for the
652 translation of a certain pool of transcripts. Thus, it will be important in future studies
653 to further dissect their specific tasks and quantify ribosomal compositions on a
654 subcellular level. Importantly, many factors of the ribosome interaction network seem
655 conserved between the green alga *Chlamydomonas* and land plants. This agrees
656 with or recent ribosome profiling study in which we observed a surprisingly conserve
657 protein synthesis output both in algae and in land plants (Trösch et al., 2018). The
658 comprehensive catalogue of chloroplast ribosome interaction network will serve as a
659 foundation for future systems biological and mechanistical studies.

660

661 **METHODS:**

662 **Cells and Culture Conditions**

663 For the construction of the Rpl5-HA (L5-HA) line, cw15 mt- strain CC4533 was used.
664 For nuclear expression of HA-tagged candidate proteins UVM4 was used (Neupert et
665 al., 2009). Cw15 CF185 was used for polysome gradients and ribosome binding
666 assays. If not stated elsewhere, cells were grown photomixotrophically in TAP
667 Medium (Harris et al., 1974) on a rotary shaker at 25 °C and under an illumination of
668 50-60 $\mu\text{moles of photons m}^{-2}\text{s}^{-1}$. For polysome analyses, cells were grown under 30
669 $\mu\text{moles of photons m}^{-2}\text{s}^{-1}$. For experiments with FA crosslink, cells were grown in
670 HAP-Medium containing 20 mM HEPES (Mettler et al., 2014). Cell densities were
671 determined using a Z2 Coulter Counter (Beckman Coulter) or estimated from OD750
672 measurement for CC4533 strains.

673 **Plasmid Construction and Genomic integration**

674 Genomic integration of the triple HA-tag coding sequence (CDS) at the 3' end of the
675 *rpl5* gene: the *rpl5* CDS including 800 bp of the 5'UTR and 195 bp of the 3'UTR was
676 amplified from genomic DNA and inserted via HiFi DNA Assembly (NEB) into *Clal*-
677 digested pUCatpXaadA (Goldschmidt-Clermont, 1991), giving the construct upstream
678 of the *aadA* resistance marker. Subsequently, additional 913 bp of the *rpl5* 3'UTR
679 were added downstream of the marker by HiFi DNA Assembly into the *NotI/XbaI*-
680 digested construct. Triple HA-tag was introduced by PCR with oligos 453 and 454
681 (Supplemental Table 2) and subsequent ligation, giving pFW182. pFW182 was
682 transformed into the chloroplast via biolistic transformation with a home-build helium-
683 driven particle gun adapted from the design of Finer et al. 1992, according to (Fischer
684 et al., 1996). After transformation, plates were incubated at 25 °C in constant light at
685 30 $\mu\text{moles of photons m}^{-2}\text{s}^{-1}$, and positive clones were selected by multiple rounds of
686 screening on increasing spectinomycin concentrations (200-1000 $\mu\text{g/mL}$). Cloning of
687 HA-tagged cpNAT1 was achieved with the MoClo strategy (Crozet et al., 2018), see
688 Supplemental Methods. For heterologous expression of cpNAT1, the coding
689 sequence of Cre14.g614750 (lacking the sequence for the putative N-terminal 57
690 amino-acid transit peptide) was synthesized (IDT) and cloned into *NdeI/EcoRI*
691 digested pTyb21 (NEB) giving pFW214. Protein expression and purification of
692 cpNAT1 was performed according to published protocols (Ries et al., 2017).

693 **Isolation of Affinity-Tagged Ribosomes**

694 Cells were grown in logarithmic phase and were pretreated for 5 min with 100 $\mu\text{g/mL}$
695 (*w/v*) chloramphenicol (CAP) or 100 $\mu\text{g/ml}$ (*w/v*) puromycin, respectively.
696 Formaldehyde was added to 0.37% (*v/v*) final concentration and cells were kept for
697 additional 10 min under light. Crosslinking was quenched by addition of 100 mM Tris-
698 HCl pH 8.0 for 5 min and cells were harvested via rapid cooling over plastic ice

699 cubes, and agitated until the temperature dropped to 4 °C. Cells were pelleted at
700 4000 g and 4 °C for 2 min and washed in lysis buffer (50 mM HEPES pH 8.0, 25 mM
701 KCl, 25 mM MgCl₂, 25 mM EGTA, 1 mM PMSF and 100 µg/mL CAP, 800 mM of KCl
702 and 100µg/mL puromycin instead of CAP for the high salt condition). Cells were
703 lysed in the respective lysis buffer including protease inhibitors (cOmplete™ EDTA-
704 free Protease Inhibitor Cocktail, Roche and 1 mM PMSF) by Avestine pressure
705 homogenization at 3 bar. After lysis, 1% (w/v) n-Dodecyl-beta-maltoside was added
706 and incubated for 5 min rotating at 4 °C. The lysates were precleared by 15 min
707 centrifugation at 4 °C and 15000 g and affinity purification was done with anti-HA
708 Magnetic Beads (Thermo Scientific) for 90 minutes at 4 °C and constant gentle
709 mixing. Beads were thoroughly washed three rounds with ice cold HKM-T buffer
710 containing 50 mM HEPES pH 8.0, 25 mM KCl, 25 mM MgCl₂ and 0.05% (v/v)
711 Tween20 and three rounds with the same buffer without Tween20. Proteins were
712 eluted with 2x SDS-PAGE buffer (125 mM Tris-HCl pH 6.8, 20% (v/v) glycerol, 4%
713 (w/v) SDS, 0.005% (w/v) Bromphenol blue) and incubated for 5 min at 96 °C. After
714 transfer into fresh tubes, crosslinker was reverted by additional incubation for 5 min
715 at 96 °C in the presence of 0.1 M DTT.

716 **Mass-spectrometric Analysis and Data Evaluation**

717 HA-affinity purification samples were briefly separated by 10% SDS-PAGE (until
718 samples migrated for 1 cm in the gel), bands were visualized by Colloidal coomassie
719 stain and cut into two bands per lane to separate the low molecular weight fraction
720 below 55 kDa from higher molecular weight fractions. Tryptic digest and peptide
721 elution were described before (Rohr et al., 2019). For reduction, gel pieces were
722 swollen in 40 mM Ammonium Bicarbonate (ABC) and 10 mM DTT and incubated at
723 55 °C for 15 min, followed by another 15 min at ambient temperature. The
724 supernatant was removed and for the reduction 100 mM Iodoacetamide (freshly

725 prepared) and 40 mM ammonium bicarbonate were added and incubated for 15 min
726 in the dark at ambient temperature. Again, the supernatant was removed, and the gel
727 pieces were washed with 40 mM ABC for 10 min. The gel pieces were then
728 dehydrated incubating in 100% acetonitrile followed by drying under vacuum.
729 Desalted peptides were separated on reverse phase columns (40 cm, 0.75 μ m inner
730 diameter) packed in-house with Reprosil-Pur C18-AQ 1.8 μ m resin (Dr. Maisch
731 GmbH) and directly injected into a Q Exactive HF spectrometer (Thermo Scientific).
732 A 90 min gradient of 2-95% buffer B (80% acetonitrile, 0.5% formic acid) at a
733 constant flow rate was used to elute peptides. Mass spectra were acquired in a data
734 dependent fashion using a top15 method for peptide sequencing. Raw data was
735 processed with MaxQuant Version 1.6.3.3 using a label-free algorithm (Cox et al.,
736 2014). MS/MS spectra were searched against the *Chlamydomonas* database
737 (<https://phytozome.jgi.doe.gov/pz/portal.html>).

738 **Statistical analysis**

739 MS data was analyzed with *Perseus* version 1.6.3.2. (Tyanova et al., 2016). Log₂
740 Label Free Quantification (LFQ) intensities (Supplemental Dataset 1) were filtered to
741 at least 2 valid values in one of the triplicates obtained from the HA pull-down
742 reactions. Missing values in the control samples were imputed with numbers from a
743 normal distribution with a mean and standard deviation chosen to best simulate low
744 abundance values close to the detection limit of the instrument. A modified *t*-test
745 (FDR=5%, S0=1) implemented in the *Perseus* software package was used to identify
746 proteins with significantly enriched LFQ intensity in the HA pulldown reactions
747 compared to a pulldown carried out with the untagged wild-type strain. All results are
748 listed in Supplementary Dataset 1. Subcellular localization and domain prediction for
749 the whole *Chlamydomonas* proteome were obtained by using ChloroP and PredAlgo
750 (Emanuelsson et al., 1999; Tardif et al., 2012) or the functional annotator web tool

751 (<https://github.com/CSBiology/FunctionalAnnotatorWeb>). The correlation coefficients
752 were calculated and visualized in *Perseus*. LFQ intensities were filtered and imputed
753 as described above and the correlation coefficient (R^2) was calculated using the
754 column corrDescribe GO term enrichment relation function.

755 ***In vitro* NAT activity assay**

756 To determine the activity of the cpNAT1, 3-16 μ g (81-324 pmol) of purified enzyme
757 were mixed with 0.2 mM of a custom-made peptide (GeneCust), 0.2% BSA in
758 acetylation buffer (50 mM Tris-HCl, pH 7.5, 8 mM EDTA, 1 mM DTT) and 45 μ M
759 [3 H]-acetyl-CoA (7.4 GBq/mmol, Hartmann Analytics). The reaction mix was topped
760 up to 0.1 mL with acetylation buffer and incubated at 37 °C for 0.5-2 h. Subsequently,
761 the samples were centrifuged at 1,500 *g* for 4 min. To isolate the custom-made
762 peptide, the supernatant was mixed with 0.1 mL SP sepharose (50% in 0.5 M acetic
763 acid) and incubated for 5 min while shaking. After 4 min of centrifugation at 1500 *g*,
764 the pellet was washed three times with 0.4 mL 0.5 M acetic acid and once with 0.4
765 mL 100% methanol. The amount of incorporated [3 H] label was measured with a Tri-
766 Carb 2810TR scintillation counter (PerkinElmer). The custom-made peptide
767 (MTIALGRFRWGRPVGRRRRPVRVYP) corresponds to the six N-terminal amino
768 acids of the *Arabidopsis thaliana* PS II reaction center protein D2 (ATCG00270)
769 fused to an arginine-rich sequence resembling the human adrenocorticotrophic
770 hormone (ACTH). The hydrophilic sequence facilitates peptide solubility and effective
771 enrichment via sepharose beads according to (Evjenth et al., 2009). The PS II
772 reaction center protein D2 was selected as a target based on the previously
773 elucidated substrate specificity of the plastidic N-terminal acetyltransferase NAA70
774 from *Arabidopsis* (Dinh et al., 2015). Both MTIA N-termini are conserved in
775 *Chlamydomonas* and *Arabidopsis*.

776 **Miscellaneous**

777 Immunofluorescence was described in (Ries et al., 2017). Slides were incubated with
778 antisera against HA and uL1c in 1:5000 and 1:2500 dilutions in PBS-BSA,
779 respectively. Slides were then washed twice with PBS for 10 min at 25 °C and
780 incubated in a 1:200 dilution of the tetramethylrhodamine-isothiocyanate (TRITC)-
781 labelled goat anti-rabbit antibody or fluorescein isothiocyanate (FITC) goat anti-
782 mouse antibody (Invitrogen, Thermo Fisher Scientific), respectively. Before imaging,
783 slides were rinsed 3 times with PBS and mounting solution containing DAPI
784 (Vectashield) was added. Images were taken with an Olympus BX53 microscope
785 containing the filters for TRITC and FITC and an Olympus DP26 color camera.
786 Ribosome co-sedimentation and polysome analysis was done according to Rohr et
787 al. (2019). For SDS-PAGE loading, protein samples were adjusted based on equal
788 protein concentrations determined by Bradford (Biorad) or BCA (Pierce) according to
789 the manufacturer's manual. SDS-PAGE and immunoblotting was done as published
790 before (Willmund and Schroda, 2005). Immunodetection was done with enhanced
791 chemiluminescence and the FUSION-FX7 Advance imaging system (PEQLAB). All
792 antibodies used are listed in Supplemental Table 3. *Chlamydomonas* cpNAT1 was
793 modelled with full length amino acid sequences using the SWISS-MODEL and
794 RaptorX server. The models were analyzed, and figures generated with UCSF
795 Chimera (Pettersen et al., 2004).

796 **Accession Numbers**

797 All gene numbers concise with the GenBank/EMBL data libraries are given in
798 Supplemental Dataset 1.

799 **Supplemental Data**

800 **Supplemental Figure 1: Reproducibility of AP-MS**

- 801 **Supplemental Figure 2:** Enrichment of plastidic ribosomal proteins
- 802 **Supplemental Figure 3:** Subcellular localization of identified proteins
- 803 **Supplemental Figure 4:** Conservation of ABC-F proteins
- 804 **Supplemental Figure 5:** Protein groups enriched in the L5-HA pulldown
- 805 **Supplemental Figure 6:** Control experiments for chemical crosslinking
- 806 **Supplemental Figure 7:** Nascent chain association of chloroplast chaperones
- 807 **Supplemental Figure 8:** Expression of HA-tagged cpNAT1
- 808 **Supplemental Figure 9:** Comparison of Chlamydomonas and Arabidopsis cpNAT1
- 809 **Supplemental Figure 10:** Migration of purified chloroplast cpNAT1
- 810 **Supplemental Figure 11:** *In vitro* acetyltransferase activity of purified mature
- 811 cpNAT1.
- 812 **Supplemental Table 1:** Known *trans*-acting factors
- 813 **Supplemental Table 2:** Primers used for cloning in this study
- 814 **Supplemental Table 3:** Antibodies used in this study
- 815 **Supplemental Table 4:** Parameters of the cpNAT1 model
- 816 **Supplemental Dataset 1:** Mass spectrometry results

817 **ACKNOWLEDGEMENTS**

818 We thank Jean-David Rochaix for antibodies against Rps12, Francis-Andre Wollman
819 for antibodies against AtpB, and Michael Schroda for antibodies against HSP90C,
820 HSP70B, SECA and TEF30 and for discussion on the data. We thank Karin Gries for
821 technical assistance with protein purification and cloning. This work was supported
822 by the Carl-Zeiss fellowship to F.R., the Deutsche Forschungsgemeinschaft grant
823 TRR175 to J.N. and F.W. and the Forschungsschwerpunkt BioComp to F.W.

824 **AUTHOR CONTRIBUTION**

825 L.D.W. designed and conducted experiments and wrote parts of the manuscript;
826 V.L.G., C.H., F.R., R.T., T.K., L.A. and M.W. performed experiments; S.R. and J.N.
827 helped with chloroplast transformation; M.R. and Z.S performed mass spectrometry
828 measurements; F.W. designed experiments, acquired funding and wrote the
829 manuscript.

830 **CONFLICT OF INTEREST**

831 The authors declare that they have no conflicts of financial interest concerning the
832 contents of this article.

833 **REFERENCES**

- 834 **Albus, C.A., Ruf, S., Schöttler, M.A., Lein, W., Kehr, J., and Bock, R.** (2010).
835 Y3IP1, a nucleus-encoded thylakoid protein, cooperates with the plastid-
836 encoded Ycf3 protein in photosystem I assembly of tobacco and *Arabidopsis*.
837 *Plant Cell* **22**, 2838-2855.
- 838 **Allen, J.F.** (2003). The function of genomes in bioenergetic organelles. *Philos Trans*
839 *R Soc Lond B Biol Sci* **358**, 19-37; discussion 37-18.
- 840 **Armbruster, U., Zühlke, J., Rengstl, B., Kreller, R., Makarenko, E., Rühle, T.,**
841 **Schünemann, D., Jahns, P., Weisshaar, B., Nickelsen, J., and Leister, D.**
842 (2010). The *Arabidopsis* thylakoid protein PAM68 is required for efficient D1
843 biogenesis and photosystem II assembly. *Plant Cell* **22**, 3439-3460.
- 844 **Armengod, M.E., Meseguer, S., Villarroya, M., Prado, S., Moukadiri, I., Ruiz-**
845 **Partida, R., Garzon, M.J., Navarro-Gonzalez, C., and Martinez-Zamora, A.**
846 (2014). Modification of the wobble uridine in bacterial and mitochondrial tRNAs
847 reading NNA/NNG triplets of 2-codon boxes. *RNA Biol* **11**, 1495-1507.
- 848 **Ban, N., Beckmann, R., Cate, J.H., Dinman, J.D., Dragon, F., Ellis, S.R.,**
849 **Lafontaine, D.L., Lindahl, L., Liljas, A., Lipton, J.M., McAlear, M.A.,**
850 **Moore, P.B., Noller, H.F., Ortega, J., Panse, V.G., Ramakrishnan, V.,**
851 **Spahn, C.M., Steitz, T.A., Tchorzewski, M., Tollervey, D., Warren, A.J.,**
852 **Williamson, J.R., Wilson, D., Yonath, A., and Yusupov, M.** (2014). A new
853 system for naming ribosomal proteins. *Curr Opin Struct Biol* **24**, 165-169.
- 854 **Barkan, A.** (2011). Expression of plastid genes: organelle-specific elaborations on a
855 prokaryotic scaffold. *Plant Physiol* **155**, 1520-1532.
- 856 **Barkan, A., and Small, I.** (2014). Pentatricopeptide repeat proteins in plants. *Annu*
857 *Rev Plant Biol* **65**, 415-442.
- 858 **Basu, A., and Yap, M.N.** (2017). Disassembly of the *Staphylococcus aureus*
859 hibernating 100S ribosome by an evolutionarily conserved GTPase. *Proc Natl*
860 *Acad Sci U S A* **114**, E8165-E8173.
- 861 **Beligni, M.V., Yamaguchi, K., and Mayfield, S.P.** (2004). The translational
862 apparatus of *Chlamydomonas reinhardtii* chloroplast. *Photosynth Res* **82**, 315-
863 325.

- 864 **Bienvenut, W.V., Espagne, C., Martinez, A., Majeran, W., Valot, B., Zivy, M.,**
865 **Vallon, O., Adam, Z., Meinel, T., and Giglione, C.** (2011). Dynamics of
866 post-translational modifications and protein stability in the stroma of
867 *Chlamydomonas reinhardtii* chloroplasts. *Proteomics* **11**, 1734-1750.
- 868 **Bieri, P., Leibundgut, M., Saurer, M., Boehringer, D., and Ban, N.** (2017). The
869 complete structure of the chloroplast 70S ribosome in complex with translation
870 factor pY. *Embo J* **36**, 475-486.
- 871 **Boel, G., Smith, P.C., Ning, W., Englander, M.T., Chen, B., Hashem, Y., Testa,**
872 **A.J., Fischer, J.J., Wieden, H.J., Frank, J., Gonzalez, R.L., Jr., and Hunt,**
873 **J.F.** (2014). The ABC-F protein EttA gates ribosome entry into the translation
874 elongation cycle. *Nat Struct Mol Biol* **21**, 143-151.
- 875 **Boerema, A.P., Aibara, S., Paul, B., Tobiasson, V., Kimanius, D., Forsberg, B.O.,**
876 **Wallden, K., Lindahl, E., and Amunts, A.** (2018). Structure of the chloroplast
877 ribosome with chl-RRF and hibernation-promoting factor. *Nat Plants* **4**, 212-
878 217.
- 879 **Bohne, A.V., Schwarz, C., Schotkowski, M., Lidschreiber, M., Piotrowski, M.,**
880 **Zerges, W., and Nickelsen, J.** (2013). Reciprocal regulation of protein
881 synthesis and carbon metabolism for thylakoid membrane biogenesis. *PLoS*
882 *Biol* **11**, e1001482.
- 883 **Borgese, N., and Fasana, E.** (2011). Targeting pathways of C-tail-anchored
884 proteins. *Biochim Biophys Acta* **1808**, 937-946.
- 885 **Bouchnak, I., and van Wijk, K.J.** (2019). N-Degron Pathways in Plastids. *Trends*
886 *Plant Sci* **24**, 917-926.
- 887 **Boulouis, A., Drapier, D., Razafimanantsoa, H., Wostrikoff, K., Tourasse, N.J.,**
888 **Pascal, K., Girard-Bascou, J., Vallon, O., Wollman, F.A., and Choquet, Y.**
889 (2015). Spontaneous dominant mutations in *chlamydomonas* highlight
890 ongoing evolution by gene diversification. *Plant Cell* **27**, 984-1001.
- 891 **Castello, A., Hentze, M.W., and Preiss, T.** (2015). Metabolic Enzymes Enjoying
892 New Partnerships as RNA-Binding Proteins. *Trends Endocrinol Metab* **26**,
893 746-757.
- 894 **Chotewutmontri, P., and Barkan, A.** (2016). Dynamics of chloroplast translation
895 during chloroplast differentiation in maize. *PLoS Genet* **12**, e1006106.
- 896 **Chotewutmontri, P., and Barkan, A.** (2018). Multilevel effects of light on ribosome
897 dynamics in chloroplasts program genome-wide and *psbA*-specific changes in
898 translation. *PLoS Genet* **14**, e1007555.
- 899 **Costanzo, M.C., Hogan, J.D., Cusick, M.E., Davis, B.P., Fancher, A.M., Hodges,**
900 **P.E., Kondu, P., Lengieza, C., Lew-Smith, J.E., Lingner, C., Roberg-Perez,**
901 **K.J., Tillberg, M., Brooks, J.E., and Garrels, J.I.** (2000). The yeast proteome
902 database (YPD) and *Caenorhabditis elegans* proteome database (WormPD):
903 comprehensive resources for the organization and comparison of model
904 organism protein information. *Nucleic Acids Res* **28**, 73-76.
- 905 **Cox, J., Hein, M.Y., Lubner, C.A., Paron, I., Nagaraj, N., and Mann, M.** (2014).
906 Accurate proteome-wide label-free quantification by delayed normalization and
907 maximal peptide ratio extraction, termed MaxLFQ. *Mol Cell Proteomics* **13**,
908 2513-2526.
- 909 **Crozet, P., Navarro, F.J., Willmund, F., Mehrshahi, P., Bakowski, K., Lauersen,**
910 **K.J., Perez-Perez, M.E., Auroy, P., Gorchs Rovira, A., Sauret-Gueto, S.,**
911 **Niemeyer, J., Spaniol, B., Theis, J., Trösch, R., Westrich, L.D., Vavitsas,**
912 **K., Baier, T., Hübner, W., de Carpentier, F., Cassarini, M., Danon, A.,**
913 **Henri, J., Marchand, C.H., de Mia, M., Sarkissian, K., Baulcombe, D.C.,**
914 **Peltier, G., Crespo, J.L., Kruse, O., Jensen, P.E., Schroda, M., Smith,**

- 915 **A.G., and Lemaire, S.D.** (2018). Birth of a Photosynthetic Chassis: A MoClo
916 Toolkit Enabling Synthetic Biology in the Microalga *Chlamydomonas*
917 *reinhardtii*. ACS Synth Biol **7**, 2074-2086.
- 918 **Das, G., and Varshney, U.** (2006). Peptidyl-tRNA hydrolase and its critical role in
919 protein biosynthesis. Microbiology **152**, 2191-2195.
- 920 **David, A., Netzer, N., Strader, M.B., Das, S.R., Chen, C.Y., Gibbs, J., Pierre, P.,**
921 **Bennink, J.R., and Yewdell, J.W.** (2011). RNA binding targets aminoacyl-
922 tRNA synthetases to translating ribosomes. J Biol Chem **286**, 20688-20700.
- 923 **DeMott, C.M., Majumder, S., Burz, D.S., Reverdatto, S., and Shekhtman, A.**
924 (2017). Ribosome Mediated Quinary Interactions Modulate In-Cell Protein
925 Activities. Biochemistry **56**, 4117-4126.
- 926 **Dinh, T.V., Bienvenut, W.V., Linster, E., Feldman-Salit, A., Jung, V.A., Meinel,**
927 **T., Hell, R., Giglione, C., and Wirtz, M.** (2015). Molecular identification and
928 functional characterization of the first Nalpha-acetyltransferase in plastids by
929 global acetylome profiling. Proteomics **15**, 2426-2435.
- 930 **Eberhard, S., Drapier, D., and Wollman, F.A.** (2002). Searching limiting steps in the
931 expression of chloroplast-encoded proteins: relations between gene copy
932 number, transcription, transcript abundance and translation rate in the
933 chloroplast of *Chlamydomonas reinhardtii*. Plant J **31**, 149-160.
- 934 **Emanuelsson, O., Nielsen, H., and von Heijne, G.** (1999). ChloroP, a neural
935 network-based method for predicting chloroplast transit peptides and their
936 cleavage sites. Protein Sci **8**, 978-984.
- 937 **Ero, R., Kumar, V., Su, W., and Gao, Y.G.** (2019). Ribosome protection by ABC-F
938 proteins-Molecular mechanism and potential drug design. Protein Sci **28**, 684-
939 693.
- 940 **Evjenth, R., Hole, K., Karlsen, O.A., Ziegler, M., Arnesen, T., and Lillehaug, J.R.**
941 (2009). Human Naa50p (Nat5/San) displays both protein *N alpha*- and *N*
942 *epsilon*-acetyltransferase activity. J Biol Chem **284**, 31122-31129.
- 943 **Fischer, N., Stampacchia, O., Redding, K., and Rochaix, J.D.** (1996). Selectable
944 marker recycling in the chloroplast. Mol Gen Genet **251**, 373-380.
- 945 **Gawronski, P., Jensen, P.E., Karpinski, S., Leister, D., and Scharff, L.B.** (2018).
946 Plastid ribosome pausing is induced by multiple features and is linked to
947 protein complex assembly. Plant Physiol.
- 948 **Germain, A., Herlich, S., Larom, S., Kim, S.H., Schuster, G., and Stern, D.B.**
949 (2011). Mutational analysis of Arabidopsis chloroplast polynucleotide
950 phosphorylase reveals roles for both RNase PH core domains in
951 polyadenylation, RNA 3'-end maturation and intron degradation. Plant J **67**,
952 381-394.
- 953 **Gloge, F., Becker, A.H., Kramer, G., and Bukau, B.** (2014). Co-translational
954 mechanisms of protein maturation. Curr Opin Struct Biol **24**, 24-33.
- 955 **Göhre, V., Ossenbühl, F., Crevecoeur, M., Eichacker, L.A., and Rochaix, J.D.**
956 (2006). One of two alb3 proteins is essential for the assembly of the
957 photosystems and for cell survival in *Chlamydomonas*. Plant Cell **18**, 1454-
958 1466.
- 959 **Goldschmidt-Clermont, M.** (1991). Transgenic expression of aminoglycoside
960 adenine transferase in the chloroplast: a selectable marker of site-directed
961 transformation of chlamydomonas. Nucleic Acids Res **19**, 4083-4089.
- 962 **Grahl, S., Reiter, B., Gügel, I.L., Vamvaka, E., Gandini, C., Jahns, P., Soll, J.,**
963 **Leister, D., and Rühle, T.** (2016). The *Arabidopsis* Protein CGLD11 Is
964 Required for Chloroplast ATP Synthase Accumulation. Mol Plant **9**, 885-899.

- 965 **Gray, M.W.** (1993). Origin and evolution of organelle genomes. *Curr Opin Genet Dev*
966 **3**, 884-890.
- 967 **Hammani, K., Bonnard, G., Bouchoucha, A., Gobert, A., Pinker, F., Salinas, T.,**
968 **and Giege, P.** (2014). Helical repeats modular proteins are major players for
969 organelle gene expression. *Biochimie* **100**, 141-150.
- 970 **Harris, E.H., Boynton, J.E., and Gillham, N.W.** (1974). Chloroplast ribosome
971 biogenesis in *Chlamydomonas*. Selection and characterization of mutants
972 blocked in ribosome formation. *J Cell Biol* **63**, 160-179.
- 973 **Hell, K., Neupert, W., and Stuart, R.A.** (2001). Oxa1p acts as a general membrane
974 insertion machinery for proteins encoded by mitochondrial DNA. *Embo J* **20**,
975 1281-1288.
- 976 **Hinnebusch, A.G.** (2015). Translational control 1995-2015: unveiling molecular
977 underpinnings and roles in human biology. *RNA* **21**, 636-639.
- 978 **Horita, S., Scotti, J.S., Thinnes, C., Mottaghi-Taromsari, Y.S., Thalhammer, A.,**
979 **Ge, W., Aik, W., Loenarz, C., Schofield, C.J., and McDonough, M.A.**
980 (2015). Structure of the ribosomal oxygenase OGFOD1 provides insights into
981 the regio- and stereoselectivity of prolyl hydroxylases. *Structure* **23**, 639-652.
- 982 **Hoshiyasu, S., Kohzuma, K., Yoshida, K., Fujiwara, M., Fukao, Y., Yokota, A.,**
983 **and Akashi, K.** (2013). Potential involvement of N-terminal acetylation in the
984 quantitative regulation of the epsilon subunit of chloroplast ATP synthase
985 under drought stress. *Biosci Biotechnol Biochem* **77**, 998-1007.
- 986 **Hristou, A., Gerlach, I., Stolle, D.S., Neumann, J., Bischoff, A., Dünschede, B.,**
987 **Nowaczyk, M.M., Zoschke, R., and Schünemann, D.** (2019). Ribosome-
988 associated chloroplast SRP54 enables efficient co-translational membrane
989 insertion of key photosynthetic proteins. *Plant Cell*.
- 990 **Hu, X.P., Yang, Y., and Ma, B.G.** (2015). Amino Acid Flux from Metabolic Network
991 Benefits Protein Translation: the Role of Resource Availability. *Sci Rep* **5**,
992 11113.
- 993 **Huber, M., Bienvenut, W.V., Linster, E., Stephan, I., Armbruster, L., Sticht, C.,**
994 **Layer, D.C., Lapouge, K., Meinnel, T., Sinning, I., Giglione, C., Hell, R.,**
995 **and Wirtz, M.** (2019). NatB-mediated N-terminal acetylation affects growth
996 and abiotic stress responses. *Plant Physiol*.
- 997 **Jeon, Y., Ahn, H.K., Kang, Y.W., and Pai, H.S.** (2017). Functional characterization
998 of chloroplast-targeted RbgA GTPase in higher plants. *Plant Mol Biol* **95**, 463-
999 479.
- 1000 **Ji, D.L., Lin, H., Chi, W., and Zhang, L.X.** (2012). CpLEPA is critical for chloroplast
1001 protein synthesis under suboptimal conditions in *Arabidopsis thaliana*. *PLoS*
1002 *One* **7**, e49746.
- 1003 **Kaczanowska, M., and Ryden-Aulin, M.** (2007). Ribosome biogenesis and the
1004 translation process in *Escherichia coli*. *Microbiol Mol Biol Rev* **71**, 477-494.
- 1005 **Kerr, I.D.** (2004). Sequence analysis of twin ATP binding cassette proteins involved
1006 in translational control, antibiotic resistance, and ribonuclease L inhibition.
1007 *Biochem Biophys Res Commun* **315**, 166-173.
- 1008 **Krutyholowa, R., Zakrzewski, K., and Glatt, S.** (2019). Charging the code - tRNA
1009 modification complexes. *Curr Opin Struct Biol* **55**, 138-146.
- 1010 **Lehtimäki, N., Koskela, M.M., and Mulo, P.** (2015). Posttranslational Modifications
1011 of Chloroplast Proteins: An Emerging Field. *Plant Physiol* **168**, 768-775.
- 1012 **Lezhneva, L., Kuras, R., Ephritikhine, G., and de Vitry, C.** (2008). A novel
1013 pathway of cytochrome c biogenesis is involved in the assembly of the
1014 cytochrome *b6f* complex in *arabidopsis* chloroplasts. *J Biol Chem* **283**, 24608-
1015 24616.

- 1016 **Linster, E., and Wirtz, M.** (2018). N-terminal acetylation: an essential protein
1017 modification emerges as an important regulator of stress responses. *J Exp Bot*
1018 **69**, 4555-4568.
- 1019 **Linster, E., Stephan, I., Bienvenut, W.V., Maple-Grodem, J., Myklebust, L.M.,**
1020 **Huber, M., Reichelt, M., Sticht, C., Moller, S.G., Meinel, T., Arnesen, T.,**
1021 **Giglione, C., Hell, R., and Wirtz, M.** (2015). Downregulation of N-terminal
1022 acetylation triggers ABA-mediated drought responses in *Arabidopsis*. *Nat*
1023 *Commun* **6**, 7640.
- 1024 **Maier, U.G., Zauner, S., Woehle, C., Bolte, K., Hempel, F., Allen, J.F., and Martin,**
1025 **W.F.** (2013). Massively convergent evolution for ribosomal protein gene
1026 content in plastid and mitochondrial genomes. *Genome Biol Evol* **5**, 2318-
1027 2329.
- 1028 **Majeran, W., Friso, G., Asakura, Y., Qu, X., Huang, M., Ponnala, L., Watkins,**
1029 **K.P., Barkan, A., and van Wijk, K.J.** (2012). Nucleoid-enriched proteomes in
1030 developing plastids and chloroplasts from maize leaves: a new conceptual
1031 framework for nucleoid functions. *Plant Physiol* **158**, 156-189.
- 1032 **Maul, J.E., Lilly, J.W., Cui, L., dePamphilis, C.W., Miller, W., Harris, E.H., and**
1033 **Stern, D.B.** (2002). The *Chlamydomonas reinhardtii* plastid chromosome:
1034 islands of genes in a sea of repeats. *Plant Cell* **14**, 2659-2679.
- 1035 **Mauro, V.P., and Edelman, G.M.** (2002). The ribosome filter hypothesis. *Proc Natl*
1036 *Acad Sci U S A* **99**, 12031-12036.
- 1037 **Mauro, V.P., and Edelman, G.M.** (2007). The ribosome filter redux. *Cell Cycle* **6**,
1038 2246-2251.
- 1039 **Mettler, T., Mühlhaus, T., Hemme, D., Schöttler, M.A., Rupprecht, J., Idoine, A.,**
1040 **Veyel, D., Pal, S.K., Yaneva-Roder, L., Winck, F.V., Sommer, F., Vosloh,**
1041 **D., Seiwert, B., Erban, A., Burgos, A., Arvidsson, S., Schönfelder, S.,**
1042 **Arnold, A., Günther, M., Krause, U., Lohse, M., Kopka, J., Nikoloski, Z.,**
1043 **Mueller-Roeber, B., Willmitzer, L., Bock, R., Schroda, M., and Stitt, M.**
1044 (2014). Systems analysis of the response of photosynthesis, metabolism, and
1045 growth to an increase in irradiance in the photosynthetic model organism
1046 *Chlamydomonas reinhardtii*. *Plant Cell* **26**, 2310-2350.
- 1047 **Moore, M.J., Soltis, P.S., Bell, C.D., Burleigh, J.G., and Soltis, D.E.** (2010).
1048 Phylogenetic analysis of 83 plastid genes further resolves the early
1049 diversification of eudicots. *Proc Natl Acad Sci U S A* **107**, 4623-4628.
- 1050 **Murina, V., Kasari, M., Takada, H., Hinnu, M., Saha, C.K., Grimshaw, J.W., Seki,**
1051 **T., Reith, M., Putrins, M., Tenson, T., Strahl, H., Hauryliuk, V., and**
1052 **Atkinson, G.C.** (2018). ABCF ATPases Involved in Protein Synthesis,
1053 Ribosome Assembly and Antibiotic Resistance: Structural and Functional
1054 Diversification across the Tree of Life. *J Mol Biol*.
- 1055 **Neupert, J., Karcher, D., and Bock, R.** (2009). Generation of *Chlamydomonas*
1056 strains that efficiently express nuclear transgenes. *Plant J* **57**, 1140-1150.
- 1057 **Nickelsen, J., Bohne, A.-V., and Westhoff, P.** (2014). Chloroplast gene expression
1058 - translation, 49-78.
- 1059 **Nishimura, K., Ashida, H., Ogawa, T., and Yokota, A.** (2010). A DEAD box protein
1060 is required for formation of a hidden break in *Arabidopsis* chloroplast 23S
1061 rRNA. *Plant J* **63**, 766-777.
- 1062 **Owtrim, G.W.** (2013). RNA helicases: diverse roles in prokaryotic response to
1063 abiotic stress. *RNA Biol* **10**, 96-110.
- 1064 **Pechmann, S., Willmund, F., and Frydman, J.** (2013). The ribosome as a hub for
1065 protein quality control. *Mol Cell* **49**, 411-421.

- 1066 **Petrov, A.S., Bernier, C.R., Hsiao, C., Norris, A.M., Kovacs, N.A., Waterbury,**
1067 **C.C., Stepanov, V.G., Harvey, S.C., Fox, G.E., Wartell, R.M., Hud, N.V.,**
1068 **and Williams, L.D.** (2014). Evolution of the ribosome at atomic resolution.
1069 *Proc Natl Acad Sci U S A* **111**, 10251-10256.
- 1070 **Pettersen, E.F., Goddard, T.D., Huang, C.C., Couch, G.S., Greenblatt, D.M.,**
1071 **Meng, E.C., and Ferrin, T.E.** (2004). UCSF Chimera--a visualization system
1072 for exploratory research and analysis. *J Comput Chem* **25**, 1605-1612.
- 1073 **Pfalz, J., Liere, K., Kandlbinder, A., Dietz, K.J., and Oelmüller, R.** (2006). pTAC2,
1074 -6, and -12 are components of the transcriptionally active plastid chromosome
1075 that are required for plastid gene expression. *Plant Cell* **18**, 176-197.
- 1076 **Preissler, S., and Deuerling, E.** (2012). Ribosome-associated chaperones as key
1077 players in proteostasis. *Trends Biochem Sci* **37**, 274-283.
- 1078 **Qin, Y., Polacek, N., Vesper, O., Staub, E., Einfeldt, E., Wilson, D.N., and**
1079 **Nierhaus, K.H.** (2006). The highly conserved LepA is a ribosomal elongation
1080 factor that back-translocates the ribosome. *Cell* **127**, 721-733.
- 1081 **Raunser, S., Magnani, R., Huang, Z., Houtz, R.L., Trievel, R.C., Penczek, P.A.,**
1082 **and Walz, T.** (2009). Rubisco in complex with Rubisco large subunit
1083 methyltransferase. *Proc Natl Acad Sci U S A* **106**, 3160-3165.
- 1084 **Ries, F., Carius, Y., Rohr, M., Gries, K., Keller, S., Lancaster, C.R.D., and**
1085 **Willmund, F.** (2017). Structural and molecular comparison of bacterial and
1086 eukaryotic trigger factors. *Sci Rep* **7**, 10680.
- 1087 **Roberts, E., Sethi, A., Montoya, J., Woese, C.R., and Luthey-Schulten, Z.** (2008).
1088 Molecular signatures of ribosomal evolution. *Proc Natl Acad Sci U S A* **105**,
1089 13953-13958.
- 1090 **Rochaix, J.D.** (2013). Redox regulation of thylakoid protein kinases and
1091 photosynthetic gene expression. *Antioxid Redox Signal* **18**, 2184-2201.
- 1092 **Röhl, T., and van Wijk, K.J.** (2001). *In vitro* reconstitution of insertion and
1093 processing of cytochrome f in a homologous chloroplast translation system. *J*
1094 *Biol Chem* **276**, 35465-35472.
- 1095 **Rohr, M., Ries, F., Herkt, C., Gotsmann, V.L., Westrich, L.D., Gries, K., Trösch,**
1096 **R., Christmann, J., Chaux, F., Jung, M., Zimmer, D., Mühlhaus, T.,**
1097 **Sommer, F.K., Schroda, M., Keller, S., Möhlmann, T., and Willmund, F.**
1098 (2019). The role of plastidic trigger factor serving protein biogenesis in green
1099 algae and land plants. *Plant Physiol*.
- 1100 **Rowland, E., Kim, J., Bhuiyan, N.H., and van Wijk, K.J.** (2015). The Arabidopsis
1101 Chloroplast Stromal N-Terminome: Complexities of Amino-Terminal Protein
1102 Maturation and Stability. *Plant Physiol* **169**, 1881-1896.
- 1103 **Rühle, T., Razeghi, J.A., Vamvaka, E., Viola, S., Gandini, C., Kleine, T.,**
1104 **Schünemann, D., Barbato, R., Jahns, P., and Leister, D.** (2014). The
1105 Arabidopsis protein CONSERVED ONLY IN THE GREEN LINEAGE160
1106 promotes the assembly of the membranous part of the chloroplast ATP
1107 synthase. *Plant Physiol* **165**, 207-226.
- 1108 **Russell, J.B., and Cook, G.M.** (1995). Energetics of bacterial growth: balance of
1109 anabolic and catabolic reactions. *Microbiol Rev* **59**, 48-62.
- 1110 **Schuster, M., Gao, Y., Schöttler, M.A., Bock, R., and Zoschke, R.** (2019). Limited
1111 Responsiveness of Chloroplast Gene Expression during Acclimation to High
1112 Light in Tobacco. *Plant Physiol*.
- 1113 **Schwarz, C., Elles, I., Kortmann, J., Piotrowski, M., and Nickelsen, J.** (2007).
1114 Synthesis of the D2 protein of photosystem II in *Chlamydomonas* is controlled
1115 by a high molecular mass complex containing the RNA stabilization factor
1116 Nac2 and the translational activator RBP40. *Plant Cell* **19**, 3627-3639.

- 1117 **Scotti, J.S., Leung, I.K., Ge, W., Bentley, M.A., Paps, J., Kramer, H.B., Lee, J.,**
1118 **Aik, W., Choi, H., Paulsen, S.M., Bowman, L.A., Loik, N.D., Horita, S., Ho,**
1119 **C.H., Kershaw, N.J., Tang, C.M., Claridge, T.D., Preston, G.M.,**
1120 **McDonough, M.A., and Schofield, C.J.** (2014). Human oxygen sensing may
1121 have origins in prokaryotic elongation factor Tu prolyl-hydroxylation. *Proc Natl*
1122 *Acad Sci U S A* **111**, 13331-13336.
- 1123 **Shajani, Z., Sykes, M.T., and Williamson, J.R.** (2011). Assembly of bacterial
1124 ribosomes. *Annu Rev Biochem* **80**, 501-526.
- 1125 **Shen, J., Williams-Carrier, R., and Barkan, A.** (2017). PSA3, a Protein on the
1126 Stromal Face of the Thylakoid Membrane, Promotes Photosystem I
1127 Accumulation in Cooperation with the Assembly Factor PYG7. *Plant Physiol*
1128 **174**, 1850-1862.
- 1129 **Shoji, S., Dambacher, C.M., Shajani, Z., Williamson, J.R., and Schultz, P.G.**
1130 (2011). Systematic chromosomal deletion of bacterial ribosomal protein
1131 genes. *J Mol Biol* **413**, 751-761.
- 1132 **Simsek, D., Tiu, G.C., Flynn, R.A., Byeon, G.W., Leppek, K., Xu, A.F., Chang,**
1133 **H.Y., and Barna, M.** (2017). The Mammalian Ribo-interactome Reveals
1134 Ribosome Functional Diversity and Heterogeneity. *Cell* **169**, 1051-1065
1135 e1018.
- 1136 **Stein, K.C., and Frydman, J.** (2019). The stop-and-go traffic regulating protein
1137 biogenesis: How translation kinetics controls proteostasis. *J Biol Chem* **294**,
1138 2076-2084.
- 1139 **Sun, Y., and Zerges, W.** (2015). Translational regulation in chloroplasts for
1140 development and homeostasis. *Biochim Biophys Acta* **1847**, 809-820.
- 1141 **Sun, Y., Valente-Paterno, M.I., Bakhtiari, S., Law, C., Zhan, Y., and Zerges, W.**
1142 (2019). Photosystem Biogenesis Is Localized to the Translation Zone in the
1143 Chloroplast of *Chlamydomonas*. *Plant Cell*.
- 1144 **Tardif, M., Atteia, A., Specht, M., Cogne, G., Rolland, N., Brugiere, S., Hippler,**
1145 **M., Ferro, M., Bruley, C., Peltier, G., Vallon, O., and Cournac, L.** (2012).
1146 PredAlgo: a new subcellular localization prediction tool dedicated to green
1147 algae. *Mol Biol Evol* **29**, 3625-3639.
- 1148 **Teter, S.A., Houry, W.A., Ang, D., Tradler, T., Rockabrand, D., Fischer, G., Blum,**
1149 **P., Georgopoulos, C., and Hartl, F.U.** (1999). Polypeptide flux through
1150 bacterial Hsp70: DnaK cooperates with trigger factor in chaperoning nascent
1151 chains. *Cell* **97**, 755-765.
- 1152 **Theis, J., and Schroda, M.** (2016). Revisiting the photosystem II repair cycle. *Plant*
1153 *Signal Behav* **11**, e1218587.
- 1154 **Trösch, R., and Willmund, F.** (2019). The conserved theme of ribosome
1155 hibernation: from bacteria to chloroplasts of plants. *Biol Chem* **400**, 879-893.
- 1156 **Trösch, R., Barahimipour, R., Gao, Y., Badillo-Corona, J.A., Gotsmann, V.L.,**
1157 **Zimmer, D., Mühlhaus, T., Zoschke, R., and Willmund, F.** (2018).
1158 Commonalities and differences of chloroplast translation in a green alga and
1159 land plants. *Nat Plants* **4**, 564-575.
- 1160 **Trotter, E.W., Rand, J.D., Vickerstaff, J., and Grant, C.M.** (2008). The yeast Tsa1
1161 peroxiredoxin is a ribosome-associated antioxidant. *Biochem J* **412**, 73-80.
- 1162 **Tsunasawa, S., Stewart, J.W., and Sherman, F.** (1985). Amino-terminal processing
1163 of mutant forms of yeast iso-1-cytochrome c. The specificities of methionine
1164 aminopeptidase and acetyltransferase. *J Biol Chem* **260**, 5382-5391.
- 1165 **Tyanova, S., Temu, T., Sinitcyn, P., Carlson, A., Hein, M.Y., Geiger, T., Mann, M.,**
1166 **and Cox, J.** (2016). The Perseus computational platform for comprehensive
1167 analysis of (prote)omics data. *Nat Methods* **13**, 731-740.

- 1168 **Voth, W., Schick, M., Gates, S., Li, S., Vilardi, F., Gostimskaya, I., Southworth,**
1169 **D.R., Schwappach, B., and Jakob, U.** (2014). The protein targeting factor
1170 Get3 functions as ATP-independent chaperone under oxidative stress
1171 conditions. *Mol Cell* **56**, 116-127.
- 1172 **Waudby, C.A., Dobson, C.M., and Christodoulou, J.** (2019). Nature and
1173 Regulation of Protein Folding on the Ribosome. *Trends Biochem Sci*.
- 1174 **Whitfeld, P.R., Leaver, C.J., Bottomley, W., and Atchison, B.** (1978). Low-
1175 molecular-weight (4.5S) ribonucleic acid in higher-plant chloroplast ribosomes.
1176 *Biochem J* **175**, 1103-1112.
- 1177 **Willmund, F., and Schroda, M.** (2005). HEAT SHOCK PROTEIN 90C is a bona fide
1178 Hsp90 that interacts with plastidic HSP70B in *Chlamydomonas reinhardtii*.
1179 *Plant Physiol* **138**, 2310-2322.
- 1180 **Xing, S., Mehlhorn, D.G., Wallmeroth, N., Asseck, L.Y., Kar, R., Voss, A.,**
1181 **Denninger, P., Schmidt, V.A., Schwarzländer, M., Stierhof, Y.D.,**
1182 **Grossmann, G., and Grefen, C.** (2017). Loss of GET pathway orthologs in
1183 *Arabidopsis thaliana* causes root hair growth defects and affects SNARE
1184 abundance. *Proc Natl Acad Sci U S A* **114**, E1544-E1553.
- 1185 **Young, R.E., and Purton, S.** (2016). Codon reassignment to facilitate genetic
1186 engineering and biocontainment in the chloroplast of *Chlamydomonas*
1187 *reinhardtii*. *Plant Biotechnol J* **14**, 1251-1260.
- 1188 **Ziehe, D., Dünschede, B., and Schünemann, D.** (2017). From bacteria to
1189 chloroplasts: evolution of the chloroplast SRP system. *Biol Chem* **398**, 653-
1190 661.
- 1191 **Zoschke, R., and Barkan, A.** (2015). Genome-wide analysis of thylakoid-bound
1192 ribosomes in maize reveals principles of cotranslational targeting to the
1193 thylakoid membrane. *Proc Natl Acad Sci U S A* **112**, E1678-1687.
- 1194 **Zoschke, R., and Bock, R.** (2018). Chloroplast Translation: Structural and
1195 Functional Organization, Operational Control and Regulation. *Plant Cell* **30**,
1196 745-770.
- 1197 **Zoschke, R., Watkins, K.P., and Barkan, A.** (2013). A rapid ribosome profiling
1198 method elucidates chloroplast ribosome behavior in vivo. *Plant Cell* **25**, 2265-
1199 2275.
- 1200 **Zybailov, B., Rutschow, H., Friso, G., Rudella, A., Emanuelsson, O., Sun, Q.,**
1201 **and van Wijk, K.J.** (2008). Sorting signals, N-terminal modifications and
1202 abundance of the chloroplast proteome. *PLoS One* **3**, e1994.
- 1203

1204

1205 **FIGURE LEGENDS**

1206 **Figure 1: Endogenous tagging of chloroplast encoded Rpl5**

1207 (A) Surface-plot model of the chloroplast ribosome based on PDB file 5MMM (Bieri et
1208 al., 2017). Ribosomal RNA is colored in light and dark grey, ribosomal proteins of the
1209 30S and 50S are highlighted in purple and turquoise, respectively. Rpl5 is highlighted
1210 in green with the surface exposed C-terminal 10 amino acids in red. (B) Design of the

1211 constructed DNA cassette for introduction of a 3xHA tag at the endogenous plastome
1212 locus of *rpl5* via homologous recombination. Correct integration was tested by PCR
1213 with oligos covering the 3'-coding sequence of *rpl5* and the adjacent resistance
1214 marker *aadA* (#1). The homoplasmic state of transformants was verified via PCR with
1215 oligos covering the 3'-coding sequence of *rpl5* and the 3' UTR of *rpl5*, separating the
1216 *rpl5* coding sequence from *AadA* (#2). Immunoblot with HA and RbcL antisera shows
1217 expression of tagged Rpl5. (C) Photoautotrophic growth test indicates that function of
1218 L5-HA tagged ribosomes are not impaired. Cells were spotted in a dilution series on
1219 HMP agar and incubated for seven days at 25 °C and constant illumination at 30
1220 $\mu\text{mol photons m}^{-2} \text{s}^{-1}$ (n=4). (D) Polysome analysis of the L5-HA tagged strain and
1221 immunoblotting of sucrose gradient fractions with anti-HA antibody shows that L5-HA
1222 is integrated into monosomes and polysomes. As controls, uL1c and uS11c were
1223 blotted in the sucrose gradient fractions with the respective antibodies. Expected
1224 positions of unassembled subunits including monosomes and polysomes in the
1225 gradient are illustrated by cartoons above the blots (n=3).

1226

1227 **Figure 2: Proteomics identification of the chloroplast ribosome network**
1228 **proteins**

1229 (A) Schematic workflow of the affinity purification-mass spectrometry approach.
1230 Experiments with L5-HA strains and the respective untagged WT were done in
1231 parallel. Before harvest, translation was arrested by addition of chloramphenicol and
1232 formaldehyde crosslinking *in vivo*. Anti-HA affinity purification was performed from
1233 detergent-solubilized whole-cell lysates, depleted of cell debris. All experiments were
1234 performed in three biological replicates (for correlations see Supplemental Figure
1235 S1). (B) Test for the specific co-precipitation of functional ribosomes (anti uL1c and
1236 uS11c) and associated factors (anti TIG1 and cpSRP54) in L5-HA eluates by

1237 immunoblotting. Pulldown experiments from wild-type cells show minor background
1238 and eluates show no detectable co-elution of cytosolic ribosomes (anti uL37) (n=3).
1239 (C) Volcano plot of the p -values versus enrichment (L5-HA pulldowns over pulldowns
1240 with untagged control). The p -values were determined by two-sided t -test, a minimal
1241 fold change $S_0 = 1$, and a permutation-based FDR = 0.01, with two valid values in
1242 first group. Highlighted are the ribosomal proteins of the plastidic large 50S subunit
1243 (dark green) and the small 30S subunit (light green). Cytosolic ribosomal proteins are
1244 marked in blue. For distribution of respective LFQ values see Supplemental Figure 2
1245 (D) Volcano plot representing the predicted subcellular localization (based on the
1246 genome annotation) of proteins enriched in the L5-HA dataset compared over
1247 proteins that were unspecifically purified with untagged wild-type samples. (E)
1248 Relative number of proteins with orthologs in *Arabidopsis*, found in the L5-HA dataset
1249 (dark green). For comparison, the relative number of all *Chlamydomonas* chloroplast
1250 localized proteins with homologs in *Arabidopsis* is shown (dark grey). (F) Functional
1251 categories of chloroplast-localized proteins that were enriched in the L5-HA dataset.
1252 Absolut numbers are given. Ribosomal proteins are excluded from this plot. For
1253 annotation and categorization see Methods.

1254

1255 **Figure 3: Protein groups enriched in the pulldown**

1256 (A)-(D) Selected functional categories of proteins of the chloroplast interaction
1257 network. On the left, cartoon indicating the category. Middle, volcano plots of
1258 enrichment in the L5-HA dataset over right-sided t -test p -values. Right, distribution of
1259 the average label-free quantification values (LFQs) for the respective proteins (n=3).
1260 All values are given in \log_2 . A minimal fold change $S_0 = 1$ and a permutation-based
1261 FDR = 0.01 were used for the reduced dataset. Functional groupings are highlighted

1262 in different colors, the names of proteins specifically mentioned in the text are
1263 indicated. For additional categories see Supplemental Figure 5.

1264

1265 **Figure 4: Validation of identified proteins**

1266 Selected proteins were validated by polysome analysis of *Chlamydomonas* lysates.
1267 Top, cartoon describing the experimental setup. Prior to harvest, translation was
1268 arrested by addition of chloramphenicol and formaldehyde crosslinking. Cells were
1269 lysed in TKM buffer (50 mM Tris-HCl pH 8, 150 mM KCl, 10 mM MgCl₂, 100 µg/ml
1270 CAP/CHX 1% Triton X-100 and 1 mM DTT) and samples were depleted of cell debris
1271 by centrifugation. For dissociation of polysomes into monosomes, half of the samples
1272 were treated with 0.07 units/µg DNase I and 1.5 units/µg RNase I for 30 min at 4 °C.
1273 Control samples were incubated without enzymes for 30 min at 4 °C. 300 µg of RNA
1274 were loaded on a sucrose gradient and centrifuged for 90 min at 35,000 rpm.
1275 Sucrose gradient fractions were immunoblotted with the indicated antisera. Fractions
1276 containing monosomes or polysomes, respectively are marked above the blot (n=4).

1277

1278 **Figure 5: Characterization of the putative co-translational acting N-** 1279 **acetyltransferase**

1280 (A) Intracellular localization of HA-tagged cpNAT1 and uL1c, as representative of
1281 chloroplast ribosomes, via immunofluorescence microscopy. Images were captured
1282 from cpNAT1-HA expressing cells (NAT-HA, top row) and UVM4 recipient strain
1283 (control, bottom row). Images from left to right: immunofluorescence using antibodies
1284 against the HA tag (FITC, green) and chloroplast-resident uL1c (TRITC, red), the
1285 merge of FITC and TRITC, and bright field (BF). The putative translation zone is
1286 marked with an arrow. Similar localization patterns were observed in 97 of 154 cells
1287 (63%). (B) Ribosome co-sedimentation assays and enrichment of cpNAT1 in the

1288 ribosomal fraction. All *Chlamydomonas* cultures were pre-treated with 100 µg/mL
1289 CAP and 100 µg/mL cycloheximide (CHX) for 5 min and harvested. For
1290 formaldehyde (FA) crosslinking, cells were incubated for 10 min with 0.37% (v/v)
1291 formaldehyde prior to harvest. All cells were lysed in buffer containing 50 mM Hepes,
1292 pH 8.0; 25 mM KCl; 10 mM MgCl₂; 0.25 x Protease-Inhibitor supplemented with 100
1293 µg/mL CAP, 100 µg/mL CHX, 200 µg/mL heparin and SupersasIn. “Puro.” release of
1294 nascent chains by addition of 1 mM puromycin in buffer without CAP. Pre-cleared cell
1295 lysates were layered on a 25% sucrose cushion (w/v) in appropriate buffer and
1296 centrifuged for 204.000 g, 20 min at 4 °C. Non-ribosome containing supernatant (S)
1297 was collected, and the ribosome pellet (R) was resuspended and separated on a
1298 12% SDS-PAGE. Note that “R” was enriched 10x compared to the sample loaded on
1299 the cushion. Ctrl = control (C) Top: Scheme representing the domains of
1300 Cre14.g614750 and its homolog from *Arabidopsis* AT4G28030. White box is
1301 chloroplast transit peptide (cTP), light grey box is unstructured N-terminal domain,
1302 dark grey box is NAT domain. Bottom: Surface (left) and ribbon (right) presentation of
1303 modelled *Chlamydomonas* cpNAT1 based on PSB 1ghe of *Pseudomonas amygdali*
1304 *pv. Tabaci*. For model parameter see Supplemental Table 4. (D) *In vitro*
1305 acetyltransferase activity of purified mature cpNAT1. Purified cpNAT1 was incubated
1306 for 1 h at 37 °C with 45 µM [³H]acetyl-CoA and 0.2 mM of the synthetic
1307 MTIALGRFRWGRPVGRRRRPVRVYP peptide. After this incubation, the peptide was
1308 separated via SP-sepharose and the amount of incorporated [³H]acetyl in the peptide
1309 was quantified by scintillation counting. The unspecific binding of [³H]acetyl-CoA to
1310 the SP-sepharose was determined with 12 µg enzyme in the absence of peptide, and
1311 was subtracted from the measurements. As a negative control, the cpNAT1 was
1312 heat-inactivated at 95 °C for 60 min (boiled). Data are presented as mean ± standard
1313 error (n=3 for each enzyme concentration).

1314

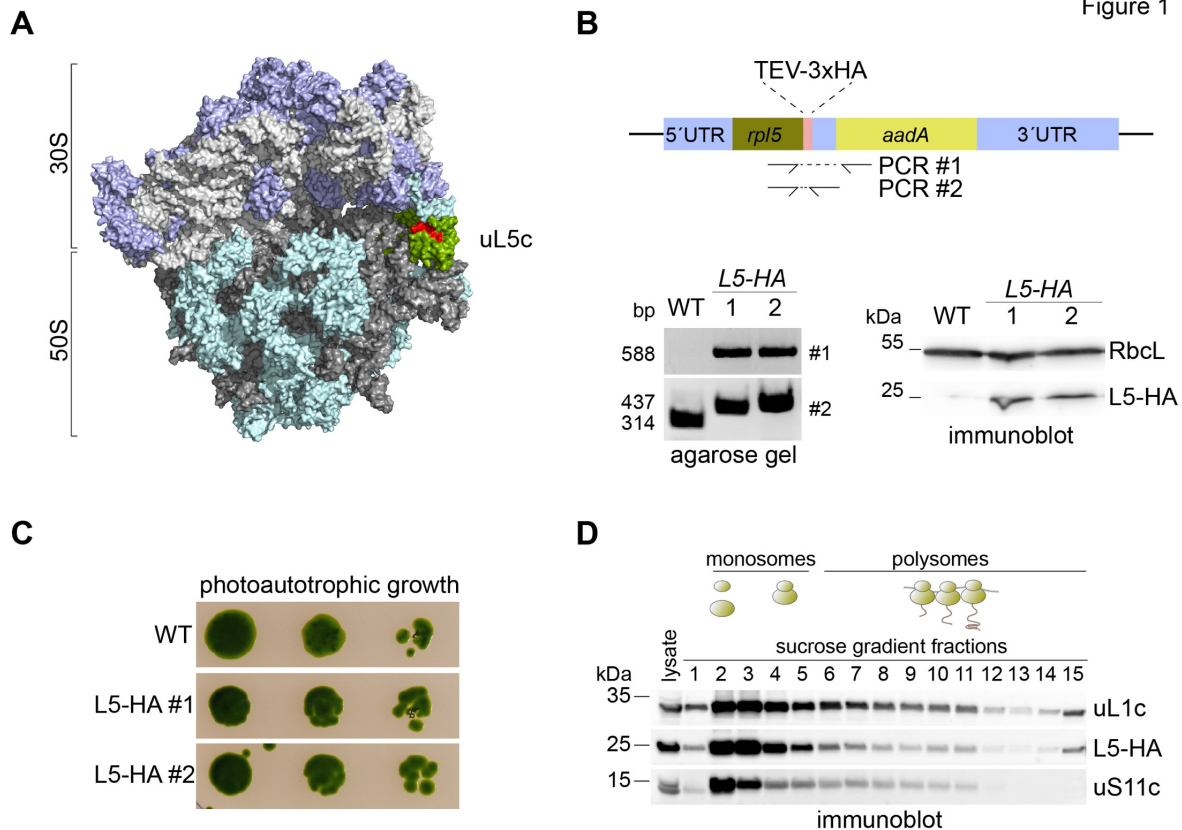


Figure 1: Endogenous tagging of chloroplast encoded Rpl5

(A) Surface-plot model of the chloroplast ribosome based on PDB file 5MMM (Bieri et al., 2017). Ribosomal RNA is colored in light and dark grey, ribosomal proteins of the 30S and 50S are highlighted in purple and turquoise, respectively. Rpl5 is highlighted in green with the surface exposed C-terminal 10 amino acids in red. (B) Design of the constructed DNA cassette for introduction of a 3xHA tag at the endogenous plastome locus of *rpl5* via homologous recombination. Correct integration was tested by PCR with oligos covering the 3'-coding sequence of *rpl5* and the adjacent resistance marker *aadA* (#1). The homoplasmic state of transformants was verified via PCR with oligos covering the 3'-coding sequence of *rpl5* and the 3' UTR of *rpl5*, separating the *rpl5* coding sequence from *AadA* (#2). Immunoblot with HA and RbcL antisera shows expression of tagged Rpl5. (C) Photoautotrophic growth test indicates that function of L5-HA tagged ribosomes are not impaired. Cells were spotted in a dilution series on HMP agar and incubated for seven days at 25 °C and constant illumination at 30 $\mu\text{mol photons m}^{-2} \text{s}^{-1}$ (n=4). (D) Polysome analysis of the L5-HA tagged strain and immunoblotting of sucrose gradient fractions with anti-HA antibody shows that L5-HA is integrated into monosomes and polysomes. As controls, uL1c and uS11c were blotted in the sucrose gradient fractions with the respective antibodies. Expected positions of unassembled subunits including monosomes and polysomes in the gradient are illustrated by cartoons above the blots (n=3).

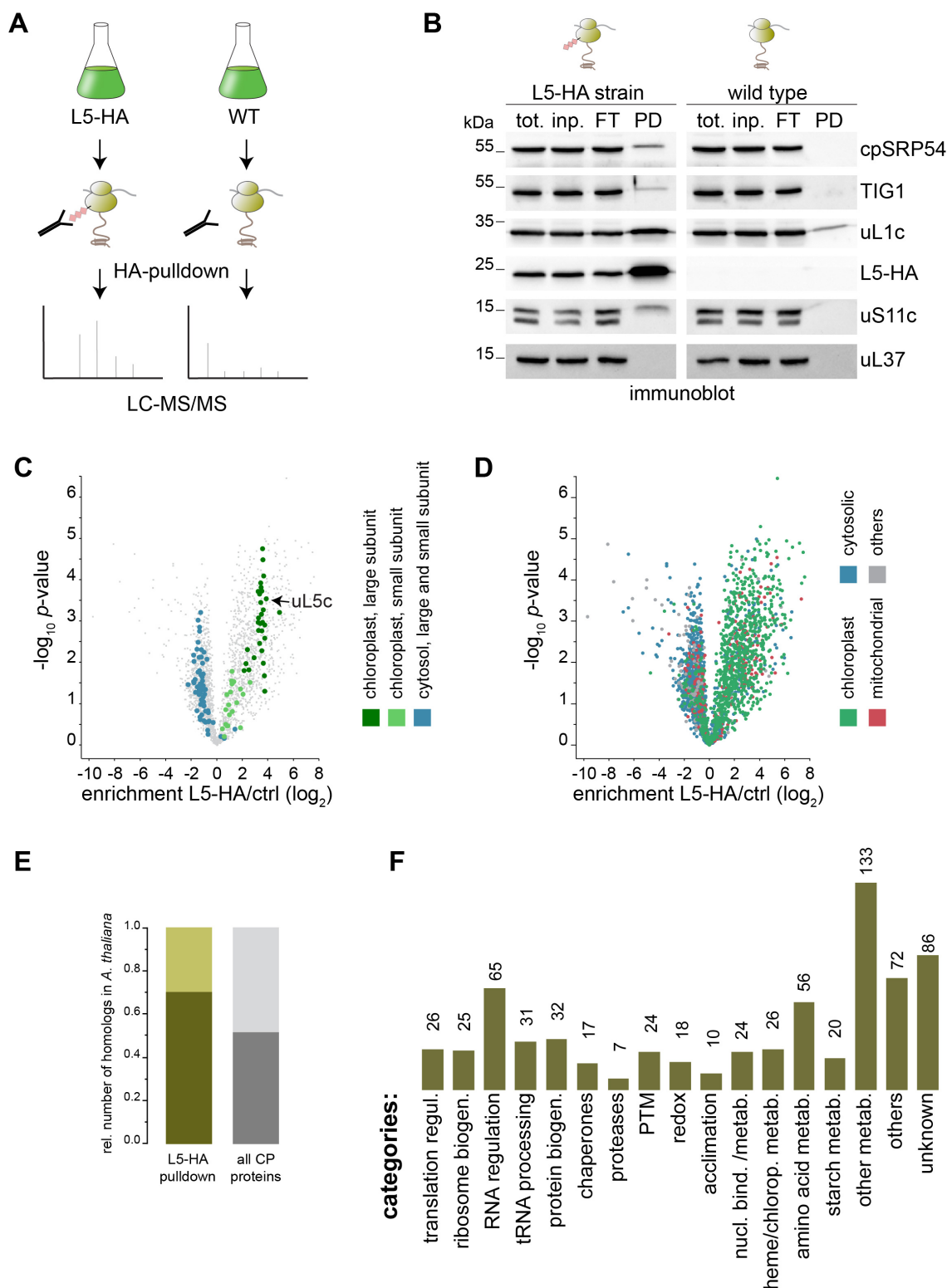
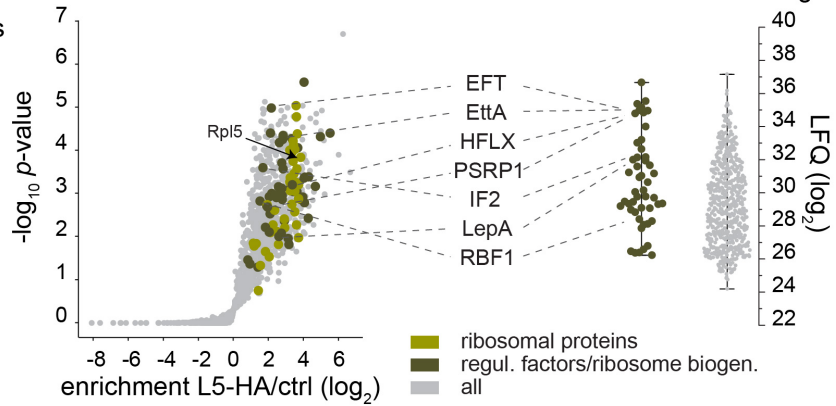
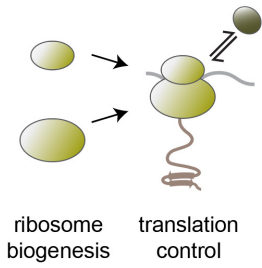


Figure 2: Proteomics identification of the chloroplast ribosome network proteins
 (A) Schematic workflow of the affinity purification-mass spectrometry approach. Experiments with L5-HA strains and the respective untagged WT were done in parallel. Before harvest, translation was arrested by addition of chloramphenicol and formaldehyde

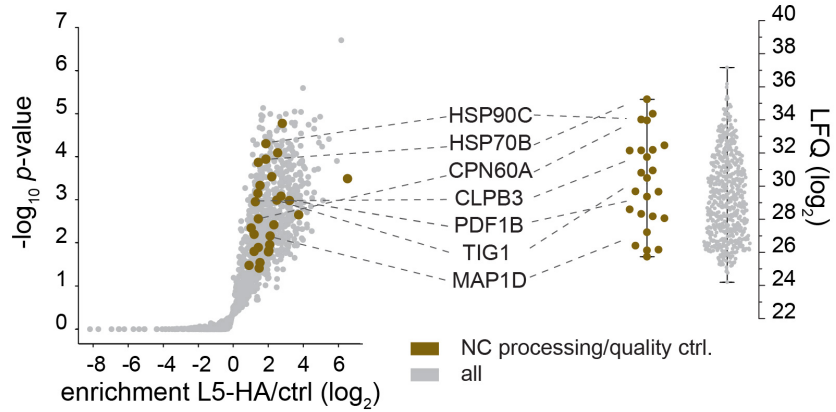
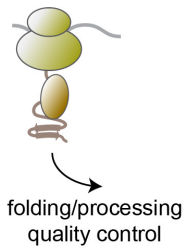
crosslinking *in vivo*. Anti-HA affinity purification was performed from detergent-solubilized whole-cell lysates, depleted of cell debris. All experiments were performed in three biological replicates (for correlations see Supplemental Figure S1). (B) Test for the specific co-precipitation of functional ribosomes (anti uL1c and uS11c) and associated factors (anti TIG1 and cpSRP54) in L5-HA eluates by immunoblotting. Pulldown experiments from wild-type cells show minor background and eluates show no detectable co-elution of cytosolic ribosomes (anti uL37) (n=3). (C) Volcano plot of the *p*-values versus enrichment (L5-HA pulldowns over pulldowns with untagged control). The *p*-values were determined by two-sided *t*-test, a minimal fold change $S_0 = 1$, and a permutation-based FDR = 0.01, with two valid values in first group. Highlighted are the ribosomal proteins of the plastidic large 50S subunit (dark green) and the small 30S subunit (light green). Cytosolic ribosomal proteins are marked in blue. For distribution of respective LFQ values see Supplemental Figure 2 (D) Volcano plot representing the predicted subcellular localization (based on the genome annotation) of proteins enriched in the L5-HA dataset compared over proteins that were unspecifically purified with untagged wild-type samples. (E) Relative number of proteins with orthologs in *Arabidopsis*, found in the L5-HA dataset (dark green). For comparison, the relative number of all *Chlamydomonas* chloroplast localized proteins with homologs in *Arabidopsis* is shown (dark grey). (F) Functional categories of chloroplast-localized proteins that were enriched in the L5-HA dataset. Absolut numbers are given. Ribosomal proteins are excluded from this plot. For annotation and categorization see Methods.

Figure 3

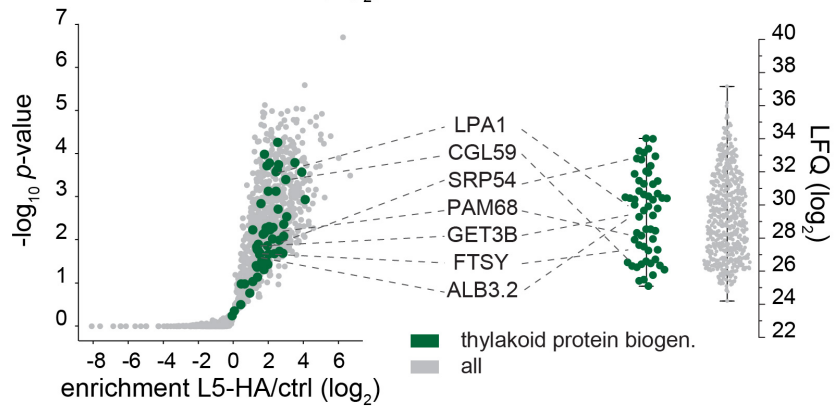
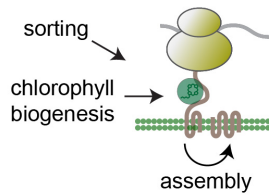
A ribosome & translation factors



B nascent chain processing



C photosystem biogenesis



D trans-acting factors

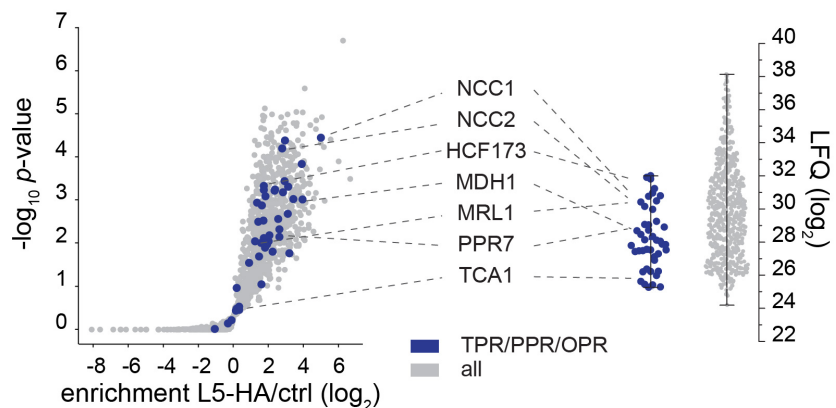
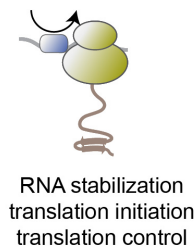


Figure 3: Protein groups enriched in the pulldown

(A)-(D) Selected functional categories of proteins of the chloroplast interaction network. On the left, cartoon indicating the category. Middle, volcano plots of enrichment in the L5-HA dataset over right-sided t-test p -values. Right, distribution of the average label-free quantification values (LFQs) for the respective proteins ($n=3$). All values are given in \log_2 . A minimal fold change $S_0 = 1$ and a permutation-based FDR = 0.01 were used for the reduced dataset. Functional groupings are highlighted in different colors, the names of proteins specifically mentioned in the text are indicated. For additional categories see Supplemental Figure 5.

Figure 4

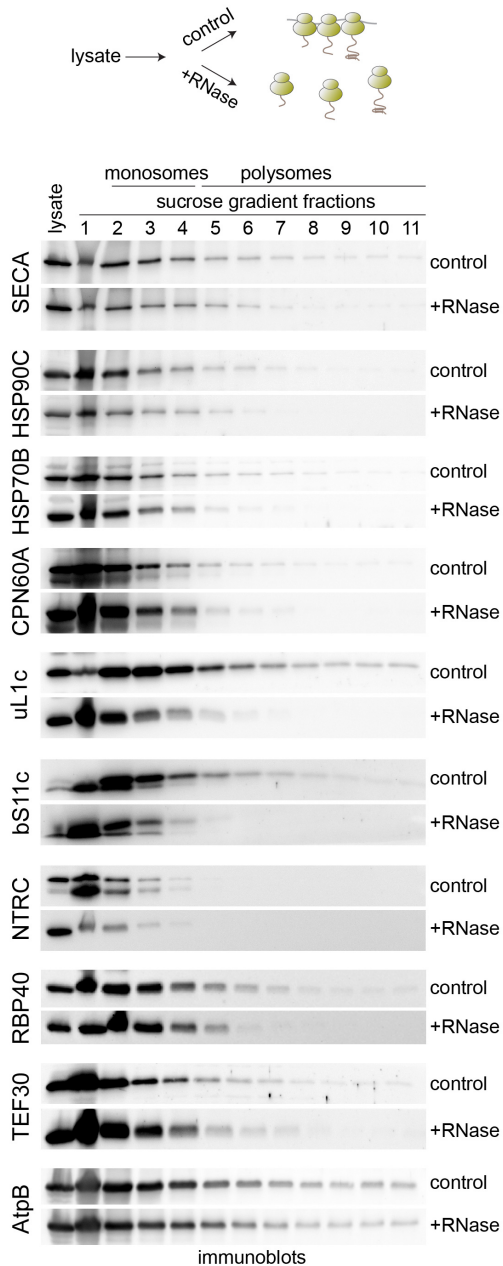


Figure 4: Validation of identified proteins

Selected proteins were validated by polysome analysis of *Chlamydomonas* lysates. Top, cartoon describing the experimental setup. Prior to harvest, translation was arrested by addition of chloramphenicol and formaldehyde crosslinking. Cells were lysed in TKM buffer (50 mM Tris-HCl pH 8, 150 mM KCl, 10 mM MgCl₂, 100 µg/ml CAP/CHX 1% Triton X-100 and 1 mM DTT) and samples were depleted of cell debris by centrifugation. For dissociation of polysomes into monosomes, half of the samples were treated with 0.07 units/µg DNase I and 1.5 units/µg RNase I for 30 min at 4 °C. Control samples were incubated without enzymes for 30 min at 4 °C. 300 µg of RNA were loaded on a sucrose gradient and centrifuged for 90 min at 35,000 rpm. Sucrose gradient fractions were immunoblotted with the indicated antisera. Fractions containing monosomes or polysomes, respectively are marked above the blot (n=4).

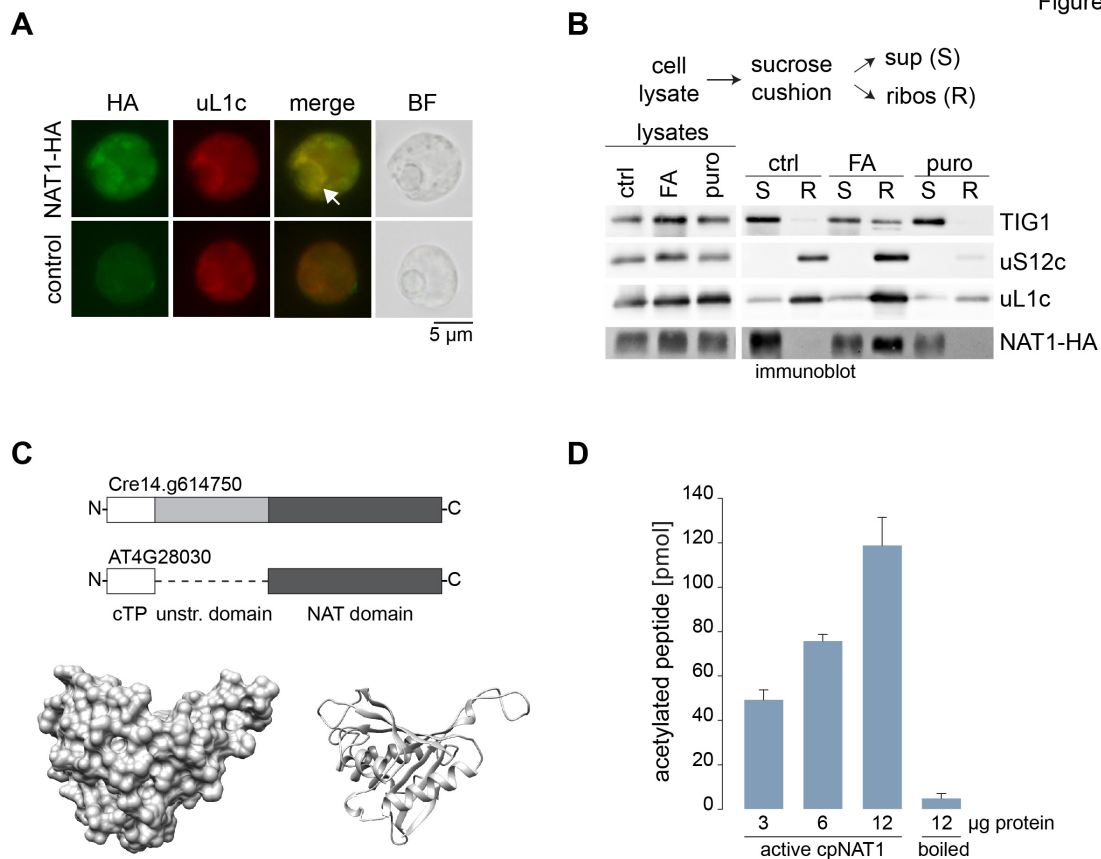


Figure 5: Characterization of the putative co-translational acting N-acetyltransferase

(A) Intracellular localization of HA-tagged cpNAT1 and uL1c, as representative of chloroplast ribosomes, via immunofluorescence microscopy. Images were captured from cpNAT1-HA expressing cells (NAT-HA, top row) and UVM4 recipient strain (control, bottom row). Images from left to right: immunofluorescence using antibodies against the HA tag (FITC, green) and chloroplast-resident uL1c (TRITC, red), the merge of FITC and TRITC, and bright field (BF). The putative translation zone is marked with an arrow. Similar localization patterns were observed in 97 of 154 cells (63%). (B) Ribosome co-sedimentation assays and enrichment of cpNAT1 in the ribosomal fraction. All *Chlamydomonas* cultures were pre-treated with 100 $\mu\text{g}/\text{mL}$ CAP and 100 $\mu\text{g}/\text{mL}$ cycloheximide (CHX) for 5 min and harvested. For formaldehyde (FA) crosslinking, cells were incubated for 10 min with 0.37% (*v/v*) formaldehyde prior to harvest. All cells were lysed in buffer containing 50 mM Hepes, pH 8.0; 25 mM KCl; 10 mM MgCl_2 ; 0.25 x Protease-Inhibitor supplemented with 100 $\mu\text{g}/\text{mL}$ CAP, 100 $\mu\text{g}/\text{mL}$ CHX, 200 $\mu\text{g}/\text{mL}$ heparin and SupersasIn. “Puro.” release of nascent chains by addition of 1 mM puromycin in buffer without CAP. Pre-cleared cell lysates were layered on a 25% sucrose cushion (*w/v*) in appropriate buffer and centrifuged for 204.000 *g*, 20 min at 4 $^\circ\text{C}$. Non-ribosome containing supernatant (S) was collected, and the ribosome pellet (R) was resuspended and separated on a 12% SDS-PAGE. Note that “R” was enriched 10x compared to the sample loaded on the cushion. Ctrl = control (C) Top: Scheme representing the domains of Cre14.g614750 and its homolog from *Arabidopsis* AT4G28030. White box is chloroplast

transit peptide (cTP), light grey box is unstructured N-terminal domain, dark grey box is NAT domain. Bottom: Surface (left) and ribbon (right) presentation of modelled *Chlamydomonas* cpNAT1 based on PSB 1ghe of *Pseudomonas amygdali* pv. *Tabaci*. For model parameter see Supplemental Table 4. (D) *In vitro* acetyltransferase activity of purified mature cpNAT1. Purified cpNAT1 was incubated for 1 h at 37 °C with 45 μM [³H]acetyl-CoA and 0.2 mM of the synthetic MTIALGRFRWGRPVGRRRRPVRVYP peptide. After this incubation, the peptide was separated via SP-sepharose and the amount of incorporated [³H]acetyl in the peptide was quantified by scintillation counting. The unspecific binding of [³H]acetyl-CoA to the SP-sepharose was determined with 12 μg enzyme in the absence of peptide, and was subtracted from the measurements. As a negative control, the cpNAT1 was heat-inactivated at 95 °C for 60 min (boiled). Data are presented as mean ± standard error (n=3 for each enzyme concentration).

Parsed Citations

Albus, C.A., Ruf, S., Schöttler, M.A., Lein, W., Kehr, J., and Bock, R. (2010). Y3IP1, a nucleus-encoded thylakoid protein, cooperates with the plastid-encoded Ycf3 protein in photosystem I assembly of tobacco and Arabidopsis. *Plant Cell* 22, 2838-2855.

Pubmed: [Author and Title](#)

Google Scholar: [Author Only Title Only Author and Title](#)

Allen, J.F. (2003). The function of genomes in bioenergetic organelles. *Philos Trans R Soc Lond B Biol Sci* 358, 19-37; discussion 37-18.

Pubmed: [Author and Title](#)

Google Scholar: [Author Only Title Only Author and Title](#)

Armbruster, U., Zühlke, J., Rengstl, B., Kreller, R., Makarenko, E., Rühle, T., Schünemann, D., Jahns, P., Weisshaar, B., Nickelsen, J., and Leister, D. (2010). The Arabidopsis thylakoid protein PAM68 is required for efficient D1 biogenesis and photosystem II assembly. *Plant Cell* 22, 3439-3460.

Pubmed: [Author and Title](#)

Google Scholar: [Author Only Title Only Author and Title](#)

Armengod, M.E., Meseguer, S., Villarroya, M., Prado, S., Moukadiri, I., Ruiz-Partida, R., Garzon, M.J., Navarro-Gonzalez, C., and Martinez-Zamora, A. (2014). Modification of the wobble uridine in bacterial and mitochondrial tRNAs reading NNA/NNG triplets of 2-codon boxes. *RNA Biol* 11, 1495-1507.

Pubmed: [Author and Title](#)

Google Scholar: [Author Only Title Only Author and Title](#)

Ban, N., Beckmann, R., Cate, J.H., Dinman, J.D., Dragon, F., Ellis, S.R., Lafontaine, D.L., Lindahl, L., Liljas, A., Lipton, J.M., McAlear, M.A., Moore, P.B., Noller, H.F., Ortega, J., Pansé, V.G., Ramakrishnan, V., Spahn, C.M., Steitz, T.A., Tchorzewski, M., Tollervey, D., Warren, A.J., Williamson, J.R., Wilson, D., Yonath, A., and Yusupov, M. (2014). A new system for naming ribosomal proteins. *Curr Opin Struct Biol* 24, 165-169.

Pubmed: [Author and Title](#)

Google Scholar: [Author Only Title Only Author and Title](#)

Barkan, A. (2011). Expression of plastid genes: organelle-specific elaborations on a prokaryotic scaffold. *Plant Physiol* 155, 1520-1532.

Pubmed: [Author and Title](#)

Google Scholar: [Author Only Title Only Author and Title](#)

Barkan, A., and Small, I. (2014). Pentatricopeptide repeat proteins in plants. *Annu Rev Plant Biol* 65, 415-442.

Pubmed: [Author and Title](#)

Google Scholar: [Author Only Title Only Author and Title](#)

Basu, A., and Yap, M.N. (2017). Disassembly of the *Staphylococcus aureus* hibernating 100S ribosome by an evolutionarily conserved GTPase. *Proc Natl Acad Sci U S A* 114, E8165-E8173.

Pubmed: [Author and Title](#)

Google Scholar: [Author Only Title Only Author and Title](#)

Beligni, M.V., Yamaguchi, K., and Mayfield, S.P. (2004). The translational apparatus of *Chlamydomonas reinhardtii* chloroplast. *Photosynth Res* 82, 315-325.

Pubmed: [Author and Title](#)

Google Scholar: [Author Only Title Only Author and Title](#)

Bienvenut, W.V., Espagne, C., Martinez, A., Majeran, W., Valot, B., Zivy, M., Vallon, O., Adam, Z., Meinel, T., and Giglione, C. (2011). Dynamics of post-translational modifications and protein stability in the stroma of *Chlamydomonas reinhardtii* chloroplasts. *Proteomics* 11, 1734-1750.

Pubmed: [Author and Title](#)

Google Scholar: [Author Only Title Only Author and Title](#)

Bieri, P., Leibundgut, M., Saurer, M., Boehringer, D., and Ban, N. (2017). The complete structure of the chloroplast 70S ribosome in complex with translation factor pY. *Embo J* 36, 475-486.

Pubmed: [Author and Title](#)

Google Scholar: [Author Only Title Only Author and Title](#)

Boel, G., Smith, P.C., Ning, W., Englander, M.T., Chen, B., Hashem, Y., Testa, A.J., Fischer, J.J., Wieden, H.J., Frank, J., Gonzalez, R.L., Jr., and Hunt, J.F. (2014). The ABC-F protein EttA gates ribosome entry into the translation elongation cycle. *Nat Struct Mol Biol* 21, 143-151.

Pubmed: [Author and Title](#)

Google Scholar: [Author Only Title Only Author and Title](#)

Boerema, A.P., Aibara, S., Paul, B., Tobiasson, V., Kimanius, D., Forsberg, B.O., Wallden, K., Lindahl, E., and Amunts, A. (2018). Structure of the chloroplast ribosome with chl-RRF and hibernation-promoting factor. *Nat Plants* 4, 212-217.

Pubmed: [Author and Title](#)

Google Scholar: [Author Only Title Only Author and Title](#)

Bohne, A.V., Schwarz, C., Schottkowski, M., Lidschreiber, M., Piotrowski, M., Zerges, W., and Nickelsen, J. (2013). Reciprocal regulation of protein synthesis and carbon metabolism for thylakoid membrane biogenesis. *PLoS Biol* 11, e1001482.

Pubmed: [Author and Title](#)

Google Scholar: [Author Only Title Only Author and Title](#)

Borgese, N., and Fasana, E. (2011). Targeting pathways of C-tail-anchored proteins. *Biochim Biophys Acta* 1808, 937-946.

Pubmed: [Author and Title](#)

Google Scholar: [Author Only Title Only Author and Title](#)

Bouchnak, I., and van Wijk, K.J. (2019). N-Degron Pathways in Plastids. *Trends Plant Sci* 24, 917-926.

Pubmed: [Author and Title](#)

Google Scholar: [Author Only Title Only Author and Title](#)

Boulouis, A., Drapier, D., Razafimanantsoa, H., Wostrickoff, K., Tourasse, N.J., Pascal, K., Girard-Bascou, J., Vallon, O., Wollman, F.A., and Choquet, Y. (2015). Spontaneous dominant mutations in *Chlamydomonas* highlight ongoing evolution by gene diversification. *Plant Cell* 27, 984-1001.

Pubmed: [Author and Title](#)

Google Scholar: [Author Only Title Only Author and Title](#)

Castello, A., Hentze, M.W., and Preiss, T. (2015). Metabolic Enzymes Enjoying New Partnerships as RNA-Binding Proteins. *Trends Endocrinol Metab* 26, 746-757.

Pubmed: [Author and Title](#)

Google Scholar: [Author Only Title Only Author and Title](#)

Chotewutmontri, P., and Barkan, A. (2016). Dynamics of chloroplast translation during chloroplast differentiation in maize. *PLoS Genet* 12, e1006106.

Pubmed: [Author and Title](#)

Google Scholar: [Author Only Title Only Author and Title](#)

Chotewutmontri, P., and Barkan, A. (2018). Multilevel effects of light on ribosome dynamics in chloroplasts program genome-wide and psbA-specific changes in translation. *PLoS Genet* 14, e1007555.

Pubmed: [Author and Title](#)

Google Scholar: [Author Only Title Only Author and Title](#)

Costanzo, M.C., Hogan, J.D., Cusick, M.E., Davis, B.P., Fancher, A.M., Hodges, P.E., Kondu, P., Lengieza, C., Lew-Smith, J.E., Lingner, C., Roberg-Perez, K.J., Tillberg, M., Brooks, J.E., and Garrels, J.I. (2000). The yeast proteome database (YPD) and *Caenorhabditis elegans* proteome database (WormPD): comprehensive resources for the organization and comparison of model organism protein information. *Nucleic Acids Res* 28, 73-76.

Pubmed: [Author and Title](#)

Google Scholar: [Author Only Title Only Author and Title](#)

Cox, J., Hein, M.Y., Luber, C.A., Paron, I., Nagaraj, N., and Mann, M. (2014). Accurate proteome-wide label-free quantification by delayed normalization and maximal peptide ratio extraction, termed MaxLFQ. *Mol Cell Proteomics* 13, 2513-2526.

Pubmed: [Author and Title](#)

Google Scholar: [Author Only Title Only Author and Title](#)

Crozet, P., Navarro, F.J., Willmund, F., Mehrshahi, P., Bakowski, K., Lauersen, K.J., Perez-Perez, M.E., Auroy, P., Gorchs Rovira, A., Sauret-Gueto, S., Niemeyer, J., Spaniol, B., Theis, J., Trösch, R., Westrich, L.D., Vavitsas, K., Baier, T., Hübner, W., de Carpentier, F., Cassarini, M., Danon, A., Henri, J., Marchand, C.H., de Mia, M., Sarkissian, K., Baulcombe, D.C., Peltier, G., Crespo, J.L., Kruse, O., Jensen, P.E., Schroda, M., Smith, A.G., and Lemaire, S.D. (2018). Birth of a Photosynthetic Chassis: A MoClo Toolkit Enabling Synthetic Biology in the Microalga *Chlamydomonas reinhardtii*. *ACS Synth Biol* 7, 2074-2086.

Pubmed: [Author and Title](#)

Google Scholar: [Author Only Title Only Author and Title](#)

Das, G., and Varshney, U. (2006). Peptidyl-tRNA hydrolase and its critical role in protein biosynthesis. *Microbiology* 152, 2191-2195.

Pubmed: [Author and Title](#)

Google Scholar: [Author Only Title Only Author and Title](#)

David, A., Netzer, N., Strader, M.B., Das, S.R., Chen, C.Y., Gibbs, J., Pierre, P., Bennink, J.R., and Yewdell, J.W. (2011). RNA binding targets aminoacyl-tRNA synthetases to translating ribosomes. *J Biol Chem* 286, 20688-20700.

Pubmed: [Author and Title](#)

Google Scholar: [Author Only Title Only Author and Title](#)

DeMott, C.M., Majumder, S., Burz, D.S., Reverdatto, S., and Shekhtman, A. (2017). Ribosome Mediated Quinary Interactions Modulate In-Cell Protein Activities. *Biochemistry* 56, 4117-4126.

Pubmed: [Author and Title](#)

Google Scholar: [Author Only Title Only Author and Title](#)

Dinh, T.V., Bienvenut, W.V., Linster, E., Feldman-Salit, A., Jung, V.A., Meinel, T., Hell, R., Giglione, C., and Wirtz, M. (2015). Molecular identification and functional characterization of the first Nalpha-acetyltransferase in plastids by global acetylome profiling. *Proteomics* 15, 2426-2435.

Pubmed: [Author and Title](#)

Google Scholar: [Author Only Title Only Author and Title](#)

Eberhard, S., Drapier, D., and Wollman, F.A. (2002). Searching limiting steps in the expression of chloroplast-encoded proteins: relations between gene copy number, transcription, transcript abundance and translation rate in the chloroplast of *Chlamydomonas reinhardtii*. *Plant J* 31, 149-160.

Pubmed: [Author and Title](#)

Google Scholar: [Author Only](#) [Title Only](#) [Author and Title](#)

Emanuelsson, O., Nielsen, H., and von Heijne, G. (1999). ChloroP, a neural network-based method for predicting chloroplast transit peptides and their cleavage sites. *Protein Sci* 8, 978-984.

Pubmed: [Author and Title](#)

Google Scholar: [Author Only](#) [Title Only](#) [Author and Title](#)

Ero, R., Kumar, V., Su, W., and Gao, Y.G. (2019). Ribosome protection by ABC-F proteins-Molecular mechanism and potential drug design. *Protein Sci* 28, 684-693.

Pubmed: [Author and Title](#)

Google Scholar: [Author Only](#) [Title Only](#) [Author and Title](#)

Evjenth, R., Hole, K., Karlsen, O.A., Ziegler, M., Arnesen, T., and Lillehaug, J.R. (2009). Human Naa50p (Nat5/San) displays both protein N alpha- and N epsilon-acetyltransferase activity. *J Biol Chem* 284, 31122-31129.

Pubmed: [Author and Title](#)

Google Scholar: [Author Only](#) [Title Only](#) [Author and Title](#)

Fischer, N., Stampacchia, O., Redding, K., and Rochaix, J.D. (1996). Selectable marker recycling in the chloroplast. *Mol Gen Genet* 251, 373-380.

Pubmed: [Author and Title](#)

Google Scholar: [Author Only](#) [Title Only](#) [Author and Title](#)

Gawronski, P., Jensen, P.E., Karpinski, S., Leister, D., and Scharff, L.B. (2018). Plastid ribosome pausing is induced by multiple features and is linked to protein complex assembly. *Plant Physiol*.

Pubmed: [Author and Title](#)

Google Scholar: [Author Only](#) [Title Only](#) [Author and Title](#)

Germain, A., Herlich, S., Larom, S., Kim, S.H., Schuster, G., and Stern, D.B. (2011). Mutational analysis of Arabidopsis chloroplast polynucleotide phosphorylase reveals roles for both RNase PH core domains in polyadenylation, RNA 3'-end maturation and intron degradation. *Plant J* 67, 381-394.

Pubmed: [Author and Title](#)

Google Scholar: [Author Only](#) [Title Only](#) [Author and Title](#)

Gloge, F., Becker, A.H., Kramer, G., and Bukau, B. (2014). Co-translational mechanisms of protein maturation. *Curr Opin Struct Biol* 24, 24-33.

Pubmed: [Author and Title](#)

Google Scholar: [Author Only](#) [Title Only](#) [Author and Title](#)

Göhre, V., Ossenbühl, F., Crevecoeur, M., Eichacker, L.A., and Rochaix, J.D. (2006). One of two alb3 proteins is essential for the assembly of the photosystems and for cell survival in Chlamydomonas. *Plant Cell* 18, 1454-1466.

Pubmed: [Author and Title](#)

Google Scholar: [Author Only](#) [Title Only](#) [Author and Title](#)

Goldschmidt-Clermont, M. (1991). Transgenic expression of aminoglycoside adenine transferase in the chloroplast: a selectable marker of site-directed transformation of chlamydomonas. *Nucleic Acids Res* 19, 4083-4089.

Pubmed: [Author and Title](#)

Google Scholar: [Author Only](#) [Title Only](#) [Author and Title](#)

Grahl, S., Reiter, B., Gügel, I.L., Vamvaka, E., Gandini, C., Jahns, P., Soll, J., Leister, D., and Rühle, T. (2016). The Arabidopsis Protein CGLD11 Is Required for Chloroplast ATP Synthase Accumulation. *Mol Plant* 9, 885-899.

Pubmed: [Author and Title](#)

Google Scholar: [Author Only](#) [Title Only](#) [Author and Title](#)

Gray, M.W. (1993). Origin and evolution of organelle genomes. *Curr Opin Genet Dev* 3, 884-890.

Pubmed: [Author and Title](#)

Google Scholar: [Author Only](#) [Title Only](#) [Author and Title](#)

Hammani, K., Bonnard, G., Bouchoucha, A., Gobert, A., Pinker, F., Salinas, T., and Giege, P. (2014). Helical repeats modular proteins are major players for organelle gene expression. *Biochimie* 100, 141-150.

Pubmed: [Author and Title](#)

Google Scholar: [Author Only](#) [Title Only](#) [Author and Title](#)

Harris, E.H., Boynton, J.E., and Gillham, N.W. (1974). Chloroplast ribosome biogenesis in Chlamydomonas. Selection and characterization of mutants blocked in ribosome formation. *J Cell Biol* 63, 160-179.

Pubmed: [Author and Title](#)

Google Scholar: [Author Only](#) [Title Only](#) [Author and Title](#)

Hell, K., Neupert, W., and Stuart, R.A. (2001). Oxa1p acts as a general membrane insertion machinery for proteins encoded by mitochondrial DNA. *Embo J* 20, 1281-1288.

Pubmed: [Author and Title](#)

Google Scholar: [Author Only](#) [Title Only](#) [Author and Title](#)

Hinnebusch, A.G. (2015). Translational control 1995-2015: unveiling molecular underpinnings and roles in human biology. *RNA* 21, 636-639.

Pubmed: [Author and Title](#)

Google Scholar: [Author Only](#) [Title Only](#) [Author and Title](#)

Horita, S., Scotti, J.S., Thinnis, C., Mottaghi-Taromsari, Y.S., Thalhammer, A., Ge, W., Aik, W., Loenarz, C., Schofield, C.J., and McDonough, M.A. (2015). Structure of the ribosomal oxygenase OGFOD1 provides insights into the regio- and stereoselectivity of prolyl hydroxylases. *Structure* 23, 639-652.

Pubmed: [Author and Title](#)

Google Scholar: [Author Only](#) [Title Only](#) [Author and Title](#)

Hoshiyasu, S., Kohzuma, K., Yoshida, K., Fujiwara, M., Fukao, Y., Yokota, A., and Akashi, K. (2013). Potential involvement of N-terminal acetylation in the quantitative regulation of the epsilon subunit of chloroplast ATP synthase under drought stress. *Biosci Biotechnol Biochem* 77, 998-1007.

Pubmed: [Author and Title](#)

Google Scholar: [Author Only](#) [Title Only](#) [Author and Title](#)

Hristou, A., Gerlach, I., Stolle, D.S., Neumann, J., Bischoff, A., Dünschede, B., Nowaczyk, M.M., Zoschke, R., and Schünemann, D. (2019). Ribosome-associated chloroplast SRP54 enables efficient co-translational membrane insertion of key photosynthetic proteins. *Plant Cell*.

Pubmed: [Author and Title](#)

Google Scholar: [Author Only](#) [Title Only](#) [Author and Title](#)

Hu, X.P., Yang, Y., and Ma, B.G. (2015). Amino Acid Flux from Metabolic Network Benefits Protein Translation: the Role of Resource Availability. *Sci Rep* 5, 11113.

Pubmed: [Author and Title](#)

Google Scholar: [Author Only](#) [Title Only](#) [Author and Title](#)

Huber, M., Bienvenut, W.V., Linster, E., Stephan, I., Armbruster, L., Sticht, C., Layer, D.C., Lapouge, K., Meinel, T., Sinning, I., Giglione, C., Hell, R., and Wirtz, M. (2019). NatB-mediated N-terminal acetylation affects growth and abiotic stress responses. *Plant Physiol*.

Pubmed: [Author and Title](#)

Google Scholar: [Author Only](#) [Title Only](#) [Author and Title](#)

Jeon, Y., Ahn, H.K., Kang, Y.W., and Pai, H.S. (2017). Functional characterization of chloroplast-targeted RbgA GTPase in higher plants. *Plant Mol Biol* 95, 463-479.

Pubmed: [Author and Title](#)

Google Scholar: [Author Only](#) [Title Only](#) [Author and Title](#)

Ji, D.L., Lin, H., Chi, W., and Zhang, L.X. (2012). CpLEPA is critical for chloroplast protein synthesis under suboptimal conditions in *Arabidopsis thaliana*. *PLoS One* 7, e49746.

Pubmed: [Author and Title](#)

Google Scholar: [Author Only](#) [Title Only](#) [Author and Title](#)

Kaczanowska, M., and Ryden-Aulin, M. (2007). Ribosome biogenesis and the translation process in *Escherichia coli*. *Microbiol Mol Biol Rev* 71, 477-494.

Pubmed: [Author and Title](#)

Google Scholar: [Author Only](#) [Title Only](#) [Author and Title](#)

Kerr, I.D. (2004). Sequence analysis of twin ATP binding cassette proteins involved in translational control, antibiotic resistance, and ribonuclease L inhibition. *Biochem Biophys Res Commun* 315, 166-173.

Pubmed: [Author and Title](#)

Google Scholar: [Author Only](#) [Title Only](#) [Author and Title](#)

Krutyholowa, R., Zakrzewski, K., and Glatt, S. (2019). Charging the code - tRNA modification complexes. *Curr Opin Struct Biol* 55, 138-146.

Pubmed: [Author and Title](#)

Google Scholar: [Author Only](#) [Title Only](#) [Author and Title](#)

Lehtimäki, N., Koskela, M.M., and Mulo, P. (2015). Posttranslational Modifications of Chloroplast Proteins: An Emerging Field. *Plant Physiol* 168, 768-775.

Pubmed: [Author and Title](#)

Google Scholar: [Author Only](#) [Title Only](#) [Author and Title](#)

Lezhneva, L., Kuras, R., Ephritikhine, G., and de Vitry, C. (2008). A novel pathway of cytochrome c biogenesis is involved in the assembly of the cytochrome b6f complex in *Arabidopsis* chloroplasts. *J Biol Chem* 283, 24608-24616.

Pubmed: [Author and Title](#)

Google Scholar: [Author Only](#) [Title Only](#) [Author and Title](#)

Linster, E., and Wirtz, M. (2018). N-terminal acetylation: an essential protein modification emerges as an important regulator of stress responses. *J Exp Bot* 69, 4555-4568.

Pubmed: [Author and Title](#)

Google Scholar: [Author Only](#) [Title Only](#) [Author and Title](#)

Linster, E., Stephan, I., Bienvenut, W.V., Maple-Grodem, J., Myklebust, L.M., Huber, M., Reichelt, M., Sticht, C., Moller, S.G., Meinel, T., Arnesen, T., Giglione, C., Hell, R., and Wirtz, M. (2015). Downregulation of N-terminal acetylation triggers ABA-mediated drought responses in *Arabidopsis*. *Nat Commun* 6, 7640.

Pubmed: [Author and Title](#)

Google Scholar: [Author Only](#) [Title Only](#) [Author and Title](#)

Maier, U.G., Zauner, S., Woehle, C., Bolte, K., Hempel, F., Allen, J.F., and Martin, W.F. (2013). Massively convergent evolution for ribosomal protein gene content in plastid and mitochondrial genomes. *Genome Biol Evol* 5, 2318-2329.

Pubmed: [Author and Title](#)

Google Scholar: [Author Only Title Only Author and Title](#)

Majeran, W., Friso, G., Asakura, Y., Qu, X., Huang, M., Ponnala, L., Watkins, K.P., Barkan, A., and van Wijk, K.J. (2012). Nucleoid-enriched proteomes in developing plastids and chloroplasts from maize leaves: a new conceptual framework for nucleoid functions. *Plant Physiol* 158, 156-189.

Pubmed: [Author and Title](#)

Google Scholar: [Author Only Title Only Author and Title](#)

Maul, J.E., Lilly, J.W., Cui, L., dePamphilis, C.W., Miller, W., Harris, E.H., and Stern, D.B. (2002). The *Chlamydomonas reinhardtii* plastid chromosome: islands of genes in a sea of repeats. *Plant Cell* 14, 2659-2679.

Pubmed: [Author and Title](#)

Google Scholar: [Author Only Title Only Author and Title](#)

Mauro, V.P., and Edelman, G.M. (2002). The ribosome filter hypothesis. *Proc Natl Acad Sci U S A* 99, 12031-12036.

Pubmed: [Author and Title](#)

Google Scholar: [Author Only Title Only Author and Title](#)

Mauro, V.P., and Edelman, G.M. (2007). The ribosome filter redux. *Cell Cycle* 6, 2246-2251.

Pubmed: [Author and Title](#)

Google Scholar: [Author Only Title Only Author and Title](#)

Mettler, T., Mühlhaus, T., Hemme, D., Schöttler, M.A., Rupprecht, J., Idoine, A., Veyel, D., Pal, S.K., Yaneva-Roder, L., Winck, F.V., Sommer, F., Vosloh, D., Seiwert, B., Erban, A., Burgos, A., Arvidsson, S., Schönfelder, S., Arnold, A., Günther, M., Krause, U., Lohse, M., Kopka, J., Nikoloski, Z., Mueller-Roeber, B., Willmitzer, L., Bock, R., Schroda, M., and Stitt, M. (2014). Systems analysis of the response of photosynthesis, metabolism, and growth to an increase in irradiance in the photosynthetic model organism *Chlamydomonas reinhardtii*. *Plant Cell* 26, 2310-2350.

Pubmed: [Author and Title](#)

Google Scholar: [Author Only Title Only Author and Title](#)

Moore, M.J., Soltis, P.S., Bell, C.D., Burleigh, J.G., and Soltis, D.E. (2010). Phylogenetic analysis of 83 plastid genes further resolves the early diversification of eudicots. *Proc Natl Acad Sci U S A* 107, 4623-4628.

Pubmed: [Author and Title](#)

Google Scholar: [Author Only Title Only Author and Title](#)

Murina, V., Kasari, M., Takada, H., Hinnu, M., Saha, C.K., Grimshaw, J.W., Seki, T., Reith, M., Putrins, M., Tenson, T., Strahl, H., Haurlyuk, V., and Atkinson, G.C. (2018). ABCF ATPases Involved in Protein Synthesis, Ribosome Assembly and Antibiotic Resistance: Structural and Functional Diversification across the Tree of Life. *J Mol Biol*.

Pubmed: [Author and Title](#)

Google Scholar: [Author Only Title Only Author and Title](#)

Neupert, J., Karcher, D., and Bock, R. (2009). Generation of *Chlamydomonas* strains that efficiently express nuclear transgenes. *Plant J* 57, 1140-1150.

Pubmed: [Author and Title](#)

Google Scholar: [Author Only Title Only Author and Title](#)

Nickelsen, J., Bohne, A-V., and Westhoff, P. (2014). Chloroplast gene expression - translation, 49-78.

Nishimura, K., Ashida, H., Ogawa, T., and Yokota, A. (2010). A DEAD box protein is required for formation of a hidden break in *Arabidopsis* chloroplast 23S rRNA. *Plant J* 63, 766-777.

Pubmed: [Author and Title](#)

Google Scholar: [Author Only Title Only Author and Title](#)

Owtrim, G.W. (2013). RNA helicases: diverse roles in prokaryotic response to abiotic stress. *RNA Biol* 10, 96-110.

Pubmed: [Author and Title](#)

Google Scholar: [Author Only Title Only Author and Title](#)

Pechmann, S., Willmund, F., and Frydman, J. (2013). The ribosome as a hub for protein quality control. *Mol Cell* 49, 411-421.

Pubmed: [Author and Title](#)

Google Scholar: [Author Only Title Only Author and Title](#)

Petrov, A.S., Bernier, C.R., Hsiao, C., Norris, A.M., Kovacs, N.A., Waterbury, C.C., Stepanov, V.G., Harvey, S.C., Fox, G.E., Wartell, R.M., Hud, N.V., and Williams, L.D. (2014). Evolution of the ribosome at atomic resolution. *Proc Natl Acad Sci U S A* 111, 10251-10256.

Pubmed: [Author and Title](#)

Google Scholar: [Author Only Title Only Author and Title](#)

Pettersen, E.F., Goddard, T.D., Huang, C.C., Couch, G.S., Greenblatt, D.M., Meng, E.C., and Ferrin, T.E. (2004). UCSF Chimera--a visualization system for exploratory research and analysis. *J Comput Chem* 25, 1605-1612.

Pubmed: [Author and Title](#)

Google Scholar: [Author Only Title Only Author and Title](#)

Pfalz, J., Liere, K., Kandlbinder, A., Dietz, K.J., and Oelmüller, R. (2006). pTAC2, -6, and -12 are components of the transcriptionally

active plastid chromosome that are required for plastid gene expression. *Plant Cell* 18, 176-197.

Pubmed: [Author and Title](#)

Google Scholar: [Author Only Title Only Author and Title](#)

Preissler, S., and Deuerling, E. (2012). Ribosome-associated chaperones as key players in proteostasis. *Trends Biochem Sci* 37, 274-283.

Pubmed: [Author and Title](#)

Google Scholar: [Author Only Title Only Author and Title](#)

Qin, Y., Polacek, N., Vesper, O., Staub, E., Einfeldt, E., Wilson, D.N., and Nierhaus, K.H. (2006). The highly conserved LepA is a ribosomal elongation factor that back-translocates the ribosome. *Cell* 127, 721-733.

Pubmed: [Author and Title](#)

Google Scholar: [Author Only Title Only Author and Title](#)

Raunser, S., Magnani, R., Huang, Z., Houtz, R.L., Trievel, R.C., Penczek, P.A., and Walz, T. (2009). Rubisco in complex with Rubisco large subunit methyltransferase. *Proc Natl Acad Sci U S A* 106, 3160-3165.

Pubmed: [Author and Title](#)

Google Scholar: [Author Only Title Only Author and Title](#)

Ries, F., Carius, Y., Rohr, M., Gries, K., Keller, S., Lancaster, C.R.D., and Willmund, F. (2017). Structural and molecular comparison of bacterial and eukaryotic trigger factors. *Sci Rep* 7, 10680.

Pubmed: [Author and Title](#)

Google Scholar: [Author Only Title Only Author and Title](#)

Roberts, E., Sethi, A., Montoya, J., Woese, C.R., and Luthey-Schulten, Z. (2008). Molecular signatures of ribosomal evolution. *Proc Natl Acad Sci U S A* 105, 13953-13958.

Pubmed: [Author and Title](#)

Google Scholar: [Author Only Title Only Author and Title](#)

Rochaix, J.D. (2013). Redox regulation of thylakoid protein kinases and photosynthetic gene expression. *Antioxid Redox Signal* 18, 2184-2201.

Pubmed: [Author and Title](#)

Google Scholar: [Author Only Title Only Author and Title](#)

Röhl, T., and van Wijk, K.J. (2001). In vitro reconstitution of insertion and processing of cytochrome f in a homologous chloroplast translation system. *J Biol Chem* 276, 35465-35472.

Pubmed: [Author and Title](#)

Google Scholar: [Author Only Title Only Author and Title](#)

Rohr, M., Ries, F., Herkt, C., Gotsmann, V.L., Westrich, L.D., Gries, K., Trösch, R., Christmann, J., Chau, F., Jung, M., Zimmer, D., Mühlhaus, T., Sommer, F.K., Schroda, M., Keller, S., Möhlmann, T., and Willmund, F. (2019). The role of plastidic trigger factor serving protein biogenesis in green algae and land plants. *Plant Physiol*.

Pubmed: [Author and Title](#)

Google Scholar: [Author Only Title Only Author and Title](#)

Rowland, E., Kim, J., Bhuiyan, N.H., and van Wijk, K.J. (2015). The Arabidopsis Chloroplast Stroma N-Terminome: Complexities of Amino-Terminal Protein Maturation and Stability. *Plant Physiol* 169, 1881-1896.

Pubmed: [Author and Title](#)

Google Scholar: [Author Only Title Only Author and Title](#)

Rühle, T., Razeghi, J.A., Vamvaka, E., Viola, S., Gandini, C., Kleine, T., Schünemann, D., Barbato, R., Jahns, P., and Leister, D. (2014). The Arabidopsis protein CONSERVED ONLY IN THE GREEN LINEAGE160 promotes the assembly of the membranous part of the chloroplast ATP synthase. *Plant Physiol* 165, 207-226.

Pubmed: [Author and Title](#)

Google Scholar: [Author Only Title Only Author and Title](#)

Russell, J.B., and Cook, G.M. (1995). Energetics of bacterial growth: balance of anabolic and catabolic reactions. *Microbiol Rev* 59, 48-62.

Pubmed: [Author and Title](#)

Google Scholar: [Author Only Title Only Author and Title](#)

Schuster, M., Gao, Y., Schöttler, M.A., Bock, R., and Zoschke, R. (2019). Limited Responsiveness of Chloroplast Gene Expression during Acclimation to High Light in Tobacco. *Plant Physiol*.

Pubmed: [Author and Title](#)

Google Scholar: [Author Only Title Only Author and Title](#)

Schwarz, C., Elles, I., Kortmann, J., Piotrowski, M., and Nickelsen, J. (2007). Synthesis of the D2 protein of photosystem II in *Chlamydomonas* is controlled by a high molecular mass complex containing the RNA stabilization factor Nac2 and the translational activator RBP40. *Plant Cell* 19, 3627-3639.

Pubmed: [Author and Title](#)

Google Scholar: [Author Only Title Only Author and Title](#)

Scotti, J.S., Leung, I.K., Ge, W., Bentley, M.A., Paps, J., Kramer, H.B., Lee, J., Aik, W., Choi, H., Paulsen, S.M., Bowman, L.A., Loik, N.D., Horita, S., Ho, C.H., Kershaw, N.J., Tang, C.M., Claridge, T.D., Preston, G.M., McDonough, M.A., and Schofield, C.J. (2014). Human

oxygen sensing may have origins in prokaryotic elongation factor Tu prolyl-hydroxylation. *Proc Natl Acad Sci U S A* 111, 13331-13336.

Pubmed: [Author and Title](#)

Google Scholar: [Author Only Title Only Author and Title](#)

Shajani, Z., Sykes, M.T., and Williamson, J.R. (2011). Assembly of bacterial ribosomes. *Annu Rev Biochem* 80, 501-526.

Pubmed: [Author and Title](#)

Google Scholar: [Author Only Title Only Author and Title](#)

Shen, J., Williams-Carrier, R., and Barkan, A. (2017). PSA3, a Protein on the Stromal Face of the Thylakoid Membrane, Promotes Photosystem I Accumulation in Cooperation with the Assembly Factor PYG7. *Plant Physiol* 174, 1850-1862.

Pubmed: [Author and Title](#)

Google Scholar: [Author Only Title Only Author and Title](#)

Shoji, S., Dambacher, C.M., Shajani, Z., Williamson, J.R., and Schultz, P.G. (2011). Systematic chromosomal deletion of bacterial ribosomal protein genes. *J Mol Biol* 413, 751-761.

Pubmed: [Author and Title](#)

Google Scholar: [Author Only Title Only Author and Title](#)

Simsek, D., Tiu, G.C., Flynn, R.A., Byeon, G.W., Leppek, K., Xu, A.F., Chang, H.Y., and Barna, M. (2017). The Mammalian Ribosome Interactome Reveals Ribosome Functional Diversity and Heterogeneity. *Cell* 169, 1051-1065 e1018.

Pubmed: [Author and Title](#)

Google Scholar: [Author Only Title Only Author and Title](#)

Stein, K.C., and Frydman, J. (2019). The stop-and-go traffic regulating protein biogenesis: How translation kinetics controls proteostasis. *J Biol Chem* 294, 2076-2084.

Pubmed: [Author and Title](#)

Google Scholar: [Author Only Title Only Author and Title](#)

Sun, Y., and Zerges, W. (2015). Translational regulation in chloroplasts for development and homeostasis. *Biochim Biophys Acta* 1847, 809-820.

Pubmed: [Author and Title](#)

Google Scholar: [Author Only Title Only Author and Title](#)

Sun, Y., Valente-Paterno, M.I., Bakhtiari, S., Law, C., Zhan, Y., and Zerges, W. (2019). Photosystem Biogenesis Is Localized to the Translation Zone in the Chloroplast of *Chlamydomonas*. *Plant Cell*.

Pubmed: [Author and Title](#)

Google Scholar: [Author Only Title Only Author and Title](#)

Tardif, M., Atteia, A., Specht, M., Cogne, G., Rolland, N., Brugiere, S., Hippler, M., Ferro, M., Bruley, C., Peltier, G., Vallon, O., and Cournac, L. (2012). PredAlgo: a new subcellular localization prediction tool dedicated to green algae. *Mol Biol Evol* 29, 3625-3639.

Pubmed: [Author and Title](#)

Google Scholar: [Author Only Title Only Author and Title](#)

Teter, S.A., Houry, W.A., Ang, D., Tradler, T., Rockabrand, D., Fischer, G., Blum, P., Georgopoulos, C., and Hartl, F.U. (1999). Polypeptide flux through bacterial Hsp70: DnaK cooperates with trigger factor in chaperoning nascent chains. *Cell* 97, 755-765.

Pubmed: [Author and Title](#)

Google Scholar: [Author Only Title Only Author and Title](#)

Theis, J., and Schroda, M. (2016). Revisiting the photosystem II repair cycle. *Plant Signal Behav* 11, e1218587.

Pubmed: [Author and Title](#)

Google Scholar: [Author Only Title Only Author and Title](#)

Trösch, R., and Willmund, F. (2019). The conserved theme of ribosome hibernation: from bacteria to chloroplasts of plants. *Biol Chem* 400, 879-893.

Pubmed: [Author and Title](#)

Google Scholar: [Author Only Title Only Author and Title](#)

Trösch, R., Barahimpour, R., Gao, Y., Badillo-Corona, J.A., Gotsmann, V.L., Zimmer, D., Mühlhaus, T., Zoschke, R., and Willmund, F. (2018). Commonalities and differences of chloroplast translation in a green alga and land plants. *Nat Plants* 4, 564-575.

Pubmed: [Author and Title](#)

Google Scholar: [Author Only Title Only Author and Title](#)

Trotter, E.W., Rand, J.D., Vickerstaff, J., and Grant, C.M. (2008). The yeast Tsa1 peroxiredoxin is a ribosome-associated antioxidant. *Biochem J* 412, 73-80.

Pubmed: [Author and Title](#)

Google Scholar: [Author Only Title Only Author and Title](#)

Tsunasawa, S., Stewart, J.W., and Sherman, F. (1985). Amino-terminal processing of mutant forms of yeast iso-1-cytochrome c. The specificities of methionine aminopeptidase and acetyltransferase. *J Biol Chem* 260, 5382-5391.

Pubmed: [Author and Title](#)

Google Scholar: [Author Only Title Only Author and Title](#)

Tyanova, S., Temu, T., Sinitcyn, P., Carlson, A., Hein, M.Y., Geiger, T., Mann, M., and Cox, J. (2016). The Perseus computational platform for comprehensive analysis of (prote)omics data. *Nat Methods* 13, 731-740.

Pubmed: [Author and Title](#)

Google Scholar: [Author Only](#) [Title Only](#) [Author and Title](#)

Voth, W., Schick, M., Gates, S., Li, S., Vilardi, F., Gostimskaya, I., Southworth, D.R., Schwappach, B., and Jakob, U. (2014). The protein targeting factor Get3 functions as ATP-independent chaperone under oxidative stress conditions. *Mol Cell* 56, 116-127.

Pubmed: [Author and Title](#)

Google Scholar: [Author Only](#) [Title Only](#) [Author and Title](#)

Waudby, C.A., Dobson, C.M., and Christodoulou, J. (2019). Nature and Regulation of Protein Folding on the Ribosome. *Trends Biochem Sci.*

Pubmed: [Author and Title](#)

Google Scholar: [Author Only](#) [Title Only](#) [Author and Title](#)

Whitfield, P.R., Leaver, C.J., Bottomley, W., and Atchison, B. (1978). Low-molecular-weight (4.5S) ribonucleic acid in higher-plant chloroplast ribosomes. *Biochem J* 175, 1103-1112.

Pubmed: [Author and Title](#)

Google Scholar: [Author Only](#) [Title Only](#) [Author and Title](#)

Willmund, F., and Schroda, M. (2005). HEAT SHOCK PROTEIN 90C is a bona fide Hsp90 that interacts with plastidic HSP70B in *Chlamydomonas reinhardtii*. *Plant Physiol* 138, 2310-2322.

Pubmed: [Author and Title](#)

Google Scholar: [Author Only](#) [Title Only](#) [Author and Title](#)

Xing, S., Mehlhorn, D.G., Wallmeroth, N., Asseck, L.Y., Kar, R., Voss, A., Denninger, P., Schmidt, V.A., Schwarzländer, M., Stierhof, Y.D., Grossmann, G., and Grefen, C. (2017). Loss of GET pathway orthologs in *Arabidopsis thaliana* causes root hair growth defects and affects SNARE abundance. *Proc Natl Acad Sci U S A* 114, E1544-E1553.

Pubmed: [Author and Title](#)

Google Scholar: [Author Only](#) [Title Only](#) [Author and Title](#)

Young, R.E., and Purton, S. (2016). Codon reassignment to facilitate genetic engineering and biocontainment in the chloroplast of *Chlamydomonas reinhardtii*. *Plant Biotechnol J* 14, 1251-1260.

Pubmed: [Author and Title](#)

Google Scholar: [Author Only](#) [Title Only](#) [Author and Title](#)

Ziehe, D., Dünschede, B., and Schünemann, D. (2017). From bacteria to chloroplasts: evolution of the chloroplast SRP system. *Biol Chem* 398, 653-661.

Pubmed: [Author and Title](#)

Google Scholar: [Author Only](#) [Title Only](#) [Author and Title](#)

Zoschke, R., and Barkan, A. (2015). Genome-wide analysis of thylakoid-bound ribosomes in maize reveals principles of cotranslational targeting to the thylakoid membrane. *Proc Natl Acad Sci U S A* 112, E1678-1687.

Pubmed: [Author and Title](#)

Google Scholar: [Author Only](#) [Title Only](#) [Author and Title](#)

Zoschke, R., and Bock, R. (2018). Chloroplast Translation: Structural and Functional Organization, Operational Control and Regulation. *Plant Cell* 30, 745-770.

Pubmed: [Author and Title](#)

Google Scholar: [Author Only](#) [Title Only](#) [Author and Title](#)

Zoschke, R., Watkins, K.P., and Barkan, A. (2013). A rapid ribosome profiling method elucidates chloroplast ribosome behavior in vivo. *Plant Cell* 25, 2265-2275.

Pubmed: [Author and Title](#)

Google Scholar: [Author Only](#) [Title Only](#) [Author and Title](#)

Zybailov, B., Rutschow, H., Friso, G., Rudella, A., Emanuelsson, O., Sun, Q., and van Wijk, K.J. (2008). Sorting signals, N-terminal modifications and abundance of the chloroplast proteome. *PLoS One* 3, e1994.

Pubmed: [Author and Title](#)

Google Scholar: [Author Only](#) [Title Only](#) [Author and Title](#)